Effect of Osmotic Stress on Barley Leaf Cuticles

Dissertation

zur

Erlangung des Doktorgrades (Dr. rer. nat.)

der

Mathematisch-Naturwissenschaftlichen Fakultät

der

Rheinischen Friedrich-Wilhelms-Universität Bonn

vorgelegt von

Nandhini Shellakkutti

aus Coimbatore, India

Bonn, 2021

Angefertigt mit Genehmigung der Mathematisch-Naturwissenschaftlichen Fakultät

der

Rheinischen Friedrich-Wilhelms-Universität Bonn.

1. Gutachter: Prof. Dr. Lukas Schreiber

2. Gutachter: Prof. Dr. Frank Hochholdinger

Tag der Promotion: 09.07.2021

Erscheinungsjahr: 2021

Contents

List of tables

List of figures

Abbreviations

ANOVA	one-way analysis of variance
BF_3/MeOH	boron trifluoride-methanol
BSTFA	N, O-bis-trimethylsilyltrifluoracetamide
EDTA	ethylenediaminetetraacetic acid
PEG	Poly Ethylene Glycol
TFs	Transcription factors
Ψ	water potential
CO_2	Carbon-dioxide
PAR	Photosynthetically active radiation
Y(II)	Quantum yield of photosystem II
ETR	Electron transfer rate
POE	Point of emergence
POI	Point of leaf insertion
DEGs	Differentially expressed genes
GO	Gene ontology
GC	Gas chromatography
FID	Flame ionization detector
MS	Mass spectrometry
SEM	Scanning electron microscope
Ø	Diameter
SI	Stomatal Index
ER	Endoplasmic reticulum
PM	Plasma membrane

1 Introduction

The evolution from aquatic life to terrestrial existence has been associated with various morphological and physiological advancement and is evident through fossil record studies. The ability of land plants to obtain mechanical support for the plant body made them resistant to biotic and abiotic stresses (Yeats & Rose, 2013). Abiotic stress, especially climate change, is the main limiting factor in modern agriculture. The most prominent abiotic stresses are increased drought, floods, air pollution and extreme temperatures which lead to food challenges in the entire world (Selvakumar et al., 2012). Global climatic changes result in rising temperatures, greater evapotranspiration and increased prevalence of drought (Campos et al., 2004). The main effects of drought are decreased water storage capacity of the soil, increased CO_2 level due to the rise of evapotranspiration, decrease in crop production and pollination and grain set could be reduced (Long & Ort, 2010). Plants are subjected to multiple stresses under field conditions during droughts, such as high light, heat and the combination of high irradiance and CO_2 deprivation. This leads for example to the down-regulation of photosynthesis (Chaves & Oliveira, 2004). Recent genomic research involving the identification of key genes responsible for abiotic stress tolerance and coupling with transgenic studies will result in improving drought-tolerant plants. For example, C-repeat binding factor (CBF), well-studied transcription factors are involved in cold and drought tolerance and overexpressing them in Arabidopsis, wheat, potato, tomato, rice, tobacco has shown an enhanced tolerance to abiotic stress (Century et al., 2008).

Barley can be grown in extreme abiotic stress environments of cold, drought, alkalinity and salinity as it is highly resistant (Kosová et al., 2014). Barley is one of the world's earliest domesticated crops ranking fourth most important cereal crop worldwide next to wheat, maize and rice. Cultivated barley (*Hordeum vulgare* L.) because of its early domestication and modern breeding strategies much of its allelic variation have been lost. *Hordeum spontaneum* (wild barley) is the ancestor of today's cultivated barley. Wild barley originates from the Fertile Crescent, which includes the regions in the middle east, which are prone to harsh summer seasons. For this reason, these populations show higher genetic variations as they are more adapted to different stress (Lakew et al., 2011). Naturally yet fully fertile crosses between the wild and

cultivated barley occur and are easily produced. Because of its occurrence of wild barley in wider habitats, the genetic diversity of wild barley can be employed for the betterment of cultivated barley (Gunasekera et al., 1994).

The effect of drought influence has led to plant water deficit and plants evolved three strategies to escape the water-deficit stress. The first approach, called drought escape is by minimizing the adverse effects by shortening the life cycle. The second approach is the drought tolerance strategy, where plants adapt their physiological functions to low water conditions. The third approach, drought avoidance is by minimizing tissue dehydration which can be achieved via stomata closure. But the stomatal closure affects the gas exchange, photosynthesis and reduces the transpiration which in turn decreases the uptake force of water and nutrients by roots (Basu et al., 2016; Kosová et al., 2014).

Plants in the natural environment overcome numerous stresses by adapting different mechanisms. As the first line of defence, they possess border tissues that control the flux of water, movement of water, nutrients, gaseous uptake and resistance to pathogens. These tissues due to structural adaptations have lipid and phenolic based barriers that are formed into polymers like suberin and cutin (Ranathunge et al., 2011). Physical adaptations by plants such as longer root systems, effectual stomatal regulation, the morphology of the leaf structures play an efficient role against drought stress (Xue et al., 2017).

1.1 Suberin and cuticles

Suberin is a complex biopolymer, an apoplastic transport barrier that is deposited in the inner layer of the cell wall of the suberizing cells or within the primary cell walls forming the Casparian strips. Uncontrolled movement of water, dissolved ions and gasses from the roots are prevented by the deposition of suberin. Formation of suberin in shoots happens and the best known is heavily suberized cork (Franke & Schreiber, 2007; Lulai et al., 1998).

In contrary to suberin, which is deposited on the inner cell surface, cuticles are deposited at the outer surface. Cuticles cover the aerial parts of the plants and are synthesized by the epidermis of the plant organs like leaves, flowers, fruits and stems. The cuticular membrane is composed of covalently linked aliphatic biopolymer cutin, cell wall carbohydrate and solvent-soluble waxes which are divided into separate

layers, epicuticular waxes coating the surface and intracuticular waxes embedded within the cutin matrix (Zeisler et al., 2017). The cuticle is divided into two domains: the cuticle proper (CP), a cutin rich domain with overlaying layer imposed with intra and extra cuticular waxes and the cuticle layer (CL) a mixture of cutin and polysaccharides (**Figure 1**). The thin cellulose-free CP is formed as the main protective layer during the development of the seeds which is generally <200 nm in thickness. The CL is a cutin rich domain with embedded polysaccharides. In higher variability of thickness, for example, some xerophytes make up to 17 µm (Bargel et al., 2006).

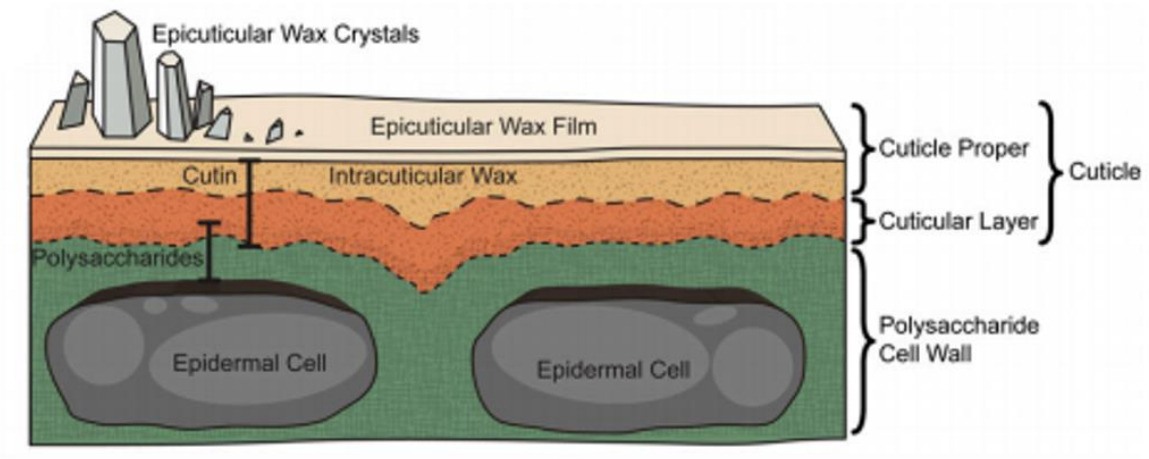

Figure 1 Structure of plant cuticles Diagrammatic representation of cuticle structure (Yeats and Rose, 2013). The cuticle is divided into two domains: the cuticle proper (CP), a cutin rich domain with overlaying layer imposed with intra and extra cuticular waxes and the cuticle layer (CL) a mixture of cutin and polysaccharides.

The deposition of cutin occurs on the outer surface of the epidermal cells. It is composed of hydroxy and hydroxy-epoxy fatty acids. Plants, in general, have C_{16} or C_{18} derivatives as a major cutin monomer with hydroxy or epoxy midchain substitutes (Wettstein-Knowels, 1993). As cutin monomers are insoluble polyester, the extraction technique vastly depends on the type of the material and the amount of sample available which includes depolymerization techniques, transesterification with BF_3 or by hydrogenolysis with $LiAlH_4$ in tetrahydrofuran (Raison, 1980). Alternatively, waxes are made of linear long-chain aliphatics with a diverse hydrocarbon chain or ring structures deposited onto or into the cutin polymer. They are extracted from the cutin by dissolving in organic solvents like chloroform or hexane.

Cutin associated wax layers offer the foremost diffusion barrier to water loss. In addition to desiccation protection, the intra- and epicuticular waxes along with the polymer, protect against the invasion of pathogens, non-stomatal water loss, ultraviolet light (UV), physical damage, prevention against movement of unwanted solutes and stress (Bi et al., 2017; Fich et al., 2016). Both intra- and epicuticular waxes differ in their composition and over the decade's different approaches have been done to extract them independently. Methods used for extracting them individually includes organic extraction for shorter (epi-) and longer times (intra-cuticular wax), removing the surface of the sample with collodion silver for chemical analysis and surface swiping with dry glass fabric and peeling of wax crystals using cryo-adhesives for epi-cuticular wax extraction (Buschhaus & Jetter, 2011). Studies show epicuticular waxes consist of long-chain aliphatics components while intracuticular waxes are composed of both triterpenoids and long-chain aliphatics. Studies on the primary leaf of barley concluded cuticular transpiration is feebly related to composition or abundance of the epicuticular wax (Larsson & Svenningsson, 1986) and from the transpiration experiment on *P. laurocerasus* proved the poor contribution of the epicuticular wax for cuticular transpiration. Thus from these studies, it is evident that the cuticular transpiration is established by the intracuticular waxes (Zeisler et al., 2018; Zeisler & Schreiber, 2016).

Plant cuticles have two different diffusion pathways for water and solutes: lateral and transverse heterogeneity (Schönherr, 2006). Leaf surfaces with stomata and trichomes contribute to lateral heterogeneity and are permeable for polar compounds. Transverse heterogeneity occurs through the cutin proper when the cuticular waxes are deposited on the outer and inner cutin polymer. Different experimental methods are used for determining the permeability of water and solute dispersion through the cuticles which include a gravimetric method, toluidine staining especially for Arabidopsis mutants or chlorophyll leaching assays (Bargel et al., 2006; Tanaka et al., 2004; Zeisler et al., 2017). The most common approach is the gravimetric method, where the intact leaves are weighed and allowed to dry out over time.

1.2 Biosynthesis of cuticular wax

The most common and prominent compounds of waxes are saturated aliphatics with very long hydrocarbon chains. These very long chains are synthesized into primary and secondary alcohols, alkanes, ketones, esters and aldehydes. Some plant species

have pentacyclic triterpenoids or tocopherols as secondary metabolites (Yeats & Rose, 2013). Cuticular wax structure and composition vary depending on the plant species.

The biosynthesis of cuticular wax begins in the plastid with the *de novo* C_{16} and C_{18} fatty acid synthesis (**Figure 2**). These fatty acids synthesized by the fatty acid synthase (FAS) complex with an acyl carrier protein (ACP) as a cofactor, acts as central intermediates for all lipid classes (Liu et al., 2019). Different types of FAS complex are required for the $C_{16/18}$ synthesis: ketoacyl ACO synthase III (KASIII) forms C_2 to C_4 chain lengths, KASI forms C_4 to C_{16} and KASII forms C_{16} and C_{18}. But they are shared by all three complexes and have no particular acyl chain length specificity. Fatty acids released from ACPs get hydrolyzed by an acyl-ACP thioesterase to transform into acyl-CoAs with help of Long-chain acyl-CoA synthetase (LACS) which are then exported to the endoplasmic reticulum (ER). In ER, C_{16} and C_{18} fatty acids are converted into very-long-chain fatty acids (VLCFAs) via fatty acid elongase (FAE) complex. FAE complex involves four sequential enzyme reactions: ß-ketoacyl-CoA synthase (KCS) condensation, reduction of ß-ketoacyl-CoA by ß-ketoacyl-CoA reductase (KCR), dehydration of ß-hydroxy acyl-CoA by ß-hydroxy acyl-CoA dehydratase (HCD) and further reduction of enoyl-CoA by enoyl-CoA reductase (ECR) (Lee & Suh, 2013).

Once elongation is complete, the wax components are produced from VLCFAs via two different pathways: acyl-reduction pathway generating primary alcohols, n-alkanes and wax esters; decarbonylation pathway producing alkanes, aldehydes, ketones and secondary alcohols. Most important of these compounds in many plant species are primary alcohols, with preferred chain lengths of C_{26} or C_{28} and in some plant species even C_{30} or C_{32}. *Brassica oleracea* and *Arabidopsis* have demonstrated as best suited for these studies as they produce higher concentrations of primary alcohols and wax esters. Investigations on *B. oleracea* by Kolattukudy, suggested a two-step process: fatty acyl-CoA reductase enzyme that reduces fatty acyl-CoA to free aldehydes and NADPH-dependent aldehyde reductase enzyme converting aldehydes to primary alcohols (Kolattukudy, 1971). Among eight FAR-like genes, CER4 which has specificity for VLCFAs is involved in the synthesis of primary alcohols (Rowland et al., 2006). Wax esters are incorporated from the CER4 forming alcohols and thus the alcohols limit the production of esters. Wax ester synthase (WS) enzymes catalyze

the ester synthesis. Investigation on *Arabidopsis* stems characterized by one of the wax synthase/acyl-CoA: diacylglycerol acyltransferase (WS/DGAT) enzyme, WSD1 which is responsible for the wax esters in some species condenses C_{16} acyl-CoA precursors and fatty alcohols forming wax esters. The aldehyde intermediates formed by FAR are simultaneously decarbonylated into alkanes by aldehyde decarbonylase which is catalyzed by CER1. The alkanes are converted into secondary alcohols and the process is catalyzed by midchain alkane hydroxylase 1 (MAH1) and further oxidation of secondary alcohol producing ketones.

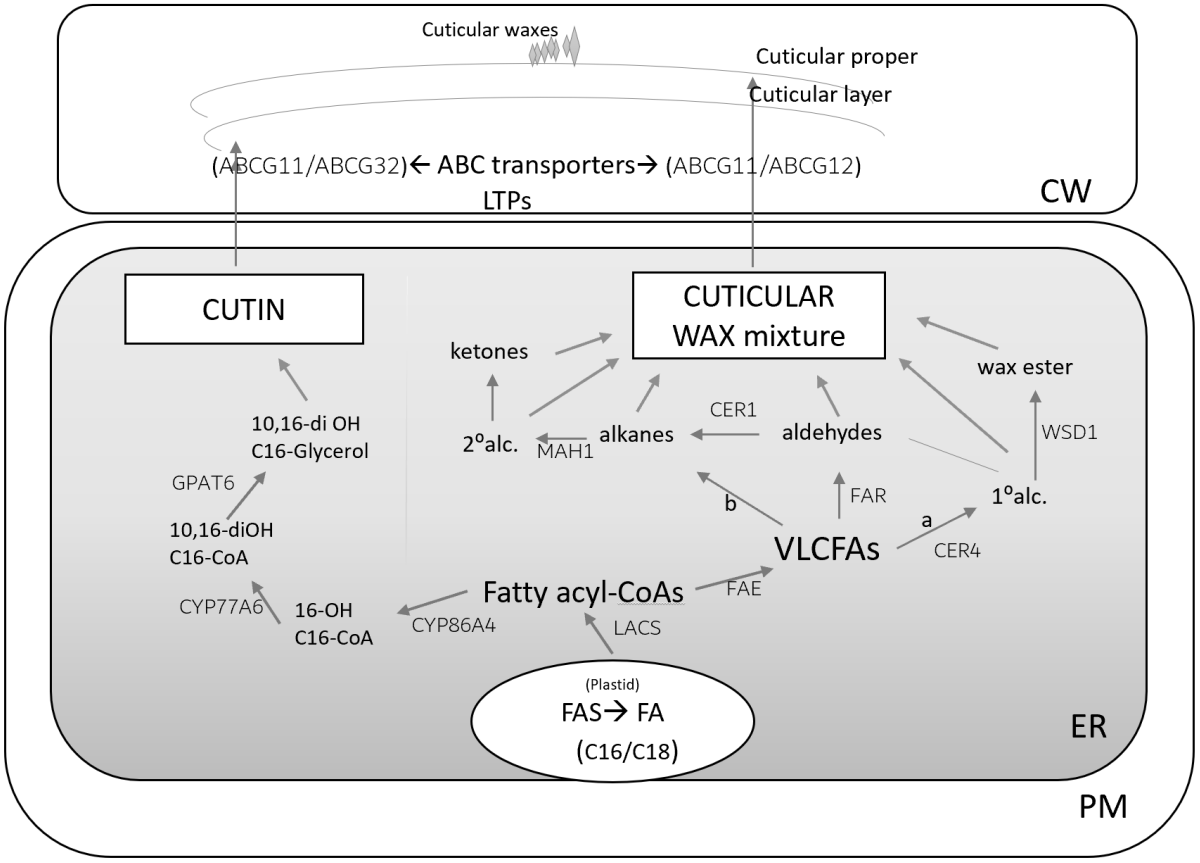

Figure 2 Overview of cutin and wax biosynthetic pathway The biosynthesis of cuticular wax/cutin begins in the plastid with the de nova C_{16} and C_{18} fatty acid synthesis. For wax synthesis, the fatty acyl-CoAs are modified into VLCFAs in ER. Later VLCFAs are converted into desired wax components via two pathways: acyl-reduction pathway and decarbonylation pathway. For cutin synthesis, the fatty acyl-CoAs undergo multiple hydroxylation and epoxidation reactions which are dependent on cytochrome P450-dependent enzymes. With help of ABC transporters and LTPs wax and cutin monomers are transported to PM then later exported to CW. ER- Endoplasmic Reticulum; PM- Plasma membrane; CW- Cell Wall; a- acyl-reduction pathway; b- decarbonylation pathway; ABC transporter– ATP binding cassette transporter; LTP- Lipid Transfer Protein. (figure modified from (Xue et al., 2017; Yeats & Rose, 2013).

Components of cuticular waxes generated in ER are transferred to the plasma membrane (PM) and then exported to the apoplast across PM and then deposited on

to the plant surface via cell walls. Transport of waxes to PM happens by either directly via the ER domains with the protoplasmic face of PM or by Golgi-mediated secretory vesicular trafficking from ER to PM. Two ATP-binding cassettes (ABC) transporters (ABCG12 and ABCG11) are involved in the export of cuticular wax (Kunst & Samuels, 2003). It has been suggested that lipid transfer proteins (LTPs) are involved in transport through the cell walls.

1.3 Biosynthesis of cutin

Cutin is composed mainly of oleic acid, 18-hydroxyoleic acid, 9,10-epoxy-18-hydroxystearic acid and 9,10,18-trihydroxystearic acid. Biosynthesis of cutin occurs by the modification of C_{16} and C_{18} carbon family generating oxygenated fatty acids-glycerol esters. The possible first step in the biosynthesis of cutin happens with the esterification of CoA yielding acyl-CoA by LACS. Hydrolysis of resultant epoxide preceded by ω-hydroxylation and epoxidation of the double bond derives oxygenated octadeca(dece)noates (Blee & Schuber, 1993). Cutin monomer oxidation steps involve cytochrome P450 enzymes. Studies on *A. thaliana* mutants *cyp86a2, -4, -8* have changed the cutin composition and structure and *cyp77a6* have lost the dihydroxy cutin monomer. Thus, the family members of CYP86A involve in terminal carbon reaction and the member of CYP77A is involved in the midchain hydroxylation reactions. The monoacylglycerol cutin monomers are generated by the enzyme glycerol-3-phosphate acyltransferase (GPAT) by transferring the acyl group from acyl-CoA to glycerol-3-phosphate. Later the cutin monomers from ER should be exported and incorporated into the cutin matrix the same as the cuticular waxes where they are transported across the PM. Similar to waxes, ABC transporters (ABCG11, ABCG13, ABCG32) involve in the cutin deposition. The export process is still least comprehended and possibly LTPs could be involved in the transport (Beisson et al., 2012; Blee & Schuber, 1993; Fich et al., 2016). The final step is the incorporation of the hydroxy acyl monomer into the polymer. But there is no clear indication of the mechanism involved. Transcription factors WIN1/SHN1 not only regulate the synthesis of the cuticular wax, but also influences the cutin composition (Kannangara et al., 2007).

1.4 Transcription factors involved in cuticle biosynthesis

Cuticular wax synthesis is limited at the transcription levels of mRNA stability. The transcription factors (TF) play an important role throughout the multiple metabolic

pathways. Transcription factors WAX INDUCER1/SHINE1 (WIN1/SHN1) belonging to the family of the AP2/ERF domain were the first to be identified and important for the wax accumulation. Overexpression of this gene results in the glossy appearance of the leaves with greater wax load (Aharoni et al., 2004). Later studies show that this gene also regulates the biosynthesis of the cutin (Kannangara et al., 2007). Studies on *Medicago truncatula* characterized *WXP1* gene of AP2 domain-containing TF increases the wax production (Zhang et al., 2005). Another important family of TF is myeloblastosis (MYB) family. Different MYB -type TFs were identified mainly in Arabidopsis includes, At*MYB*41, -16, -106, -96, -30 and from tomato SlMYB12. The Arabidopsis *MYB96* was recognized as a regulator of drought stress and their expression activates a set of genes responsible for the cuticular wax biosynthesis (Bi et al., 2016; Yeats & Rose, 2013).

1.5 Functions of cuticles

Plant cuticle offers various biological functions in terms of physical and biochemical properties among them their main function is as a barrier against excessive transpirational water loss. Cuticles were noticed in the oldest fossil of the terrestrial plants which indicates the survival of the plant's life against the dry environment (Müller & Riederer, 2005). Notably, cuticular waxes protect against water loss. Extracting the waxes, the permeability of the cuticles increases on average from 100-1000 fold (Schreiber, 2010). Studies on tomato mutant *cutin deficient 2* noticed a minimal effect on the transpiration rate with significant reductions in the cutin amount. In contrast, the same studies on tomato fruit with less reduction in the cutin amount resulted in increased transpirational rate (Fich et al., 2016). Studies on *Capsicum annuum* L. presented that cutin has no direct linkage to post-harvest water loss (Kissinger et al., 2005). In contrast, studies on barley mutant *eibi1*, show the cutin matrix is important for the cuticle to function against the water loss (Guoxiong Chen et al., 2011). These results imply rather than the cutin amount, a fully, structurally formed cutin matrix is essential for the cuticles to act as the barrier against water loss. Thus, the cutin matrix contributes to the mechanical strength and cuticular waxes against transpirational loss.

Cuticles have photoprotective properties that regulate the wavelengths of the light that penetrates the plant tissues. Cuticles associated with the phenolic compounds (like flavonoids) acts as the UV-B protection or in some species they are reflected away by

the glaucous appearance. These phenolics are also associated with antimicrobial properties (Krauss et al., 1997; Solovchenko & Merzlyak, 2003; Yeats & Rose, 2013).

Different mechanisms by the cuticles may involve against plant pathogens: cutin/wax monomers may release signals activating plant disease resistance or inhibiting the growth of pathogens on the surface (Ziv et al., 2018). Fruits and leaves evolve different strategies for defending themselves. Fruits produce a physical barrier with more amounts of cutin while leaves degrade the cutin matrix which triggers the defense response (Fich et al., 2016).

1.6 Aim of the study

Assessing the drought stress tolerance at the seedling stage is an important trait as it later affects the growth and grain yield. The leaf and root characteristics are mainly focused on during this seedling stage. The outcome of osmotic stress induced by the application of PEG8000 on barley roots was examined previously by (Kreszies et al., 2019, 2020). In the present investigation, the study was extended to aerial parts focusing on the leaf response to osmotic stress under the same condition.

Similar to suberin which prevents the uncontrolled water and ion movement in the roots, the aerial parts of the plants are covered by cuticles and they protect the shoot during the water deficit condition. The investigation was carried out on different physiological and chemical parameters of cuticles. Physiological adaptation by plants happens with less reduction in water content, immediate stomatal closure, decreased photosynthetic activity and accumulation of more compatible solutes. Subsequently, changes in wax/ cutin deposition and their gene expression pattern were studied. All the above-mentioned characteristics were measured on 12-d old cultivated barley (Hordeum vulgare spp. vulgare) and compared with wild barley (Hordeum vulgare spp. Spontaneum) as a response to osmotic stress induced by the application of PEG8000 (water potential -0.8MPa). Conclusions from these results will address if and how the cuticles help barley to cope with the water deficit conditions.

2 Materials and methods

2.1 Plant material and growth conditions

Barley seeds of cultivar Scarlett and wild accession ICB181243 (from Pakistan) were placed separately in a moisturized paper on a petri-plate to germinate in the dark at 25ºC. After three days, the germinated seeds were transferred to the aerated hydroponics system containing half-strength Hoagland solution with macro and micronutrients and water potential of -0.025 MPa (**Table 1**). The plants were grown in a climatic chamber under long-day conditions of 16h light and 8h dark at 131 $\mu m*m^{-2}*s^{-1}$, an air temperature of 23/20°C (day/night) and relative air humidity of 50 – 65%.

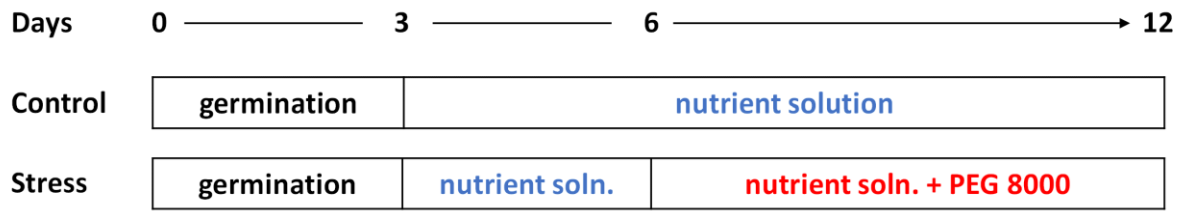

Figure 3 Experimental setup of growth conditions Three days the seeds were germinated in dark. After 3 d of germination, the seeds were transferred to hydroponics containing half-strength Hoagland solution. For stress treatment, the nutrient solution was replaced with a nutrient solution containing 25.4 % (w/w) polyethylene glycol 8000 (PEG 8000) on day 6.

Table 1 Composition of half-strength Hoagland nutrient solution.

Elements	The concentration of the stock solution	The volume of the final solution (1 Litre)
Macro-nutrients		
○ $Ca(NO_3)_2.\ 4H_2O$	1 M	1 ml
○ KNO_3	1 M	1 ml
○ KH_2PO_4	1 M	1 ml
○ $MgSO_4\ .7H_2O$	1 M	1 ml
Micro-nutrients		
○ H_3BO_3	45 mM	0.5 ml
○ MnCl2. 4 H2O	9.1 mM	0.5 ml
○ ZnSO4. 7 H2O	695 µM	0.5 ml
○ CuSO4. 5 H2O	400 µM	0.5 ml
○ $Na_2MoO_4.\ 2\ H_2O$	0.121 mM	0.5 ml
○ Fe- EDTA*	-	0.5 ml

* Fe-EDTA preparation (0.5 ml added to final solutions)
- 28 g KOH in 0.5l ddH_2O
- pH adj. to 5.5 with H_2SO_4
- add 5.2g EDTA and 3.9g $FeSO_4.7H_2O$

Six days after germination, osmotic stress was applied by reducing the water potential from -0.025 MPa to -0.8 MPa by adding 25.4% (w/w) PEG8000 to the half-strength Hoagland solution (**Figure 3**). The concentration of PEG was calculated from the formula given below which was published by (Michel, 1983). The water potential was measured by using a WP4C dew point hygrometer (Decagon device) according to the manufacturer's instructions.

$$[PEG] = {(4 - (5.16\Psi T - 560\Psi + 16)^{0.5}}\Big/{(2.58T - 280)} \qquad \text{(Michel, 1983)}$$

Where Ψ is the water potential, T is the temperature.

2.2 Stomatal transpiration

Stomatal transpiration was measured using a leaf AP4 porometer (Delta-T Devices, England). Five measurements were taken from the same leaf each day with a time gap of 30 min. The first measurement was made immediately after reducing the water potential along with the parallel controls. Leaves were randomly selected for measurements and a minimum of three biological replicates were taken along with two technical replicates. Data are the average of all five measurements from the same day.

2.3 Stomatal density and Stomatal Index

Stomatal density was obtained for both ad- and abaxial sides of leaf 1 and leaf 2 separately by Collodium imprints (nail polish imprints). Each leaf was cut into three segments and fixed to the double-sided tape. Epidermal leaf impression was prepared by coating the leaf surface with clear nail polish. The dried leaf surface was peeled off with cellotape and fixed on the microscopic slide. Leaf imprints were viewed via epifluorescence microscopy with a Zeiss AxioPlan microscope (Carl Zeiss, Germany). The images were captured with a mounted Canon EOS 600D SLR camera (Conon Inc. Tokyo, Japan). Stomatal density and epidermal cell counts were evaluated in Image J (ImageJ.net).

Stomatal index (SI) was calculated as,

$$SI\ (\%) = \frac{S}{S+E} \times 100$$

where, S is the number of stomatal cells and E is the number of epidermal cells

2.4 Residual transpiration

The water permeability of the barley leaves was determined by the gravimetric method. Twelve-day old leaves were detached from the plants, fresh weights were immediately measured using an analytical balance (Sartorius CPA225D, Goettingen, Germany) with a resolution of ± 0.01 mg. Weight loss of leaves was measured initially each 5 min for the first one hour. Later measurements were obtained every 30 min over the total time of 3.5 h. The leaves were maintained in the dark at 2% humidity and 25ºC between each measurement. The dry weight of the leaves was obtained by letting them dry overnight in the 60ºC cabinet. Minimum 4 leaves of each genotype were used for both conditions. Permeance was calculated from the formula given below,

$$P = \frac{F}{\Delta C} \qquad \text{(Niederl et al., 1998)}$$

where, P is Permeance (m s^{-1}), F is the driving force expressed per unit area and ∆C is the concentration of the water.

2.5 Light curve

Light curve measurements were done with the Pulse-amplitude modulated (PAM) chlorophyll fluorometry (Heinz Walz GmbH, Germany). Measurements were started immediately after reducing the water potential and made by exposing the same leaves to increasing actinic light illumination in a time gap of 5 min. The photosynthetic yield (II) and electron transfer rate were measured with light intensity starting from 25 µmol m^{-2} s^{-1} and increased stepwise to 820 µmol m^{-2} s^{-1} (25, 45, 66, 90, 125, 190, 285, 420, 625, 820 µmol m^{-2} s^{-1}). Leaves were randomly selected for measurements and a minimum of three biological replicates was taken along with two technical replicates.

2.6 Proline estimation

Photometric determination of proline was done for 12-d old barley leaves of both cultivars. Fresh leaves (100 mg) were harvested and immediately frozen in liquid nitrogen. Proline extraction from frozen samples by the ninhydrin method derived from

(Bates, 1973). The determined proline amount was expressed in µg g^{-1} of fresh weight. Leaves were randomly selected for measurements and a minimum of three biological replicates was taken along with two technical replicates.

2.7 Scanning Electron Microscope

The leaf surface was investigated by Scanning Electron Microscope (SEM) at the Nees Institute for biodiversity of plants, the University of Bonn, Germany. The 12-d old plants were harvested and approximately 2.5 cm of central leaf portion was cut and fixed to the aluminium stubs (ø 2.5 cm) with double-sided adhesive tape. Later the samples were dried for a minimum of 2 days over silica gel. When completely dried the samples were placed into the gold sputtering system and sputter gold for 1 min at 30 mA and voltage of 2.4 kV. This results in a thin coating of 72 nm of the gold layer. The thickness of the sputter coat was calculated from the formula given below,

$$d\ (nm) = mA\ \times kV\ \times t\ \times k$$

where, d is the thickness (nm), mA is the discharge current, kV is the voltage, t is time (min) and k is the constant.

With an accelerating voltage of 20 keV in a high vacuum, the SEM was executed and the pictures of the leaves were taken (Cambridge S 200 Stereoscan, Cambridge, UK; equipped with DISS 5 image acquisition system, Point Electronic, Halle, Germany).

2.8 Wax and cutin extraction

Leaf samples (4 cm segments, leaf 1, leaf 2) as shown in **Figure 4** were individually dipped in 2 ml of chloroform for 20 sec at room temperature. Subsequently, the dipped leaves were scanned for area determination and transferred to the vials containing chloroform: methanol (1:1) (Zeier Jurgen & Schreiber, 1997) for cutin analysis. The extract of cuticular wax was immediately spiked with 10 µg/50 mg of tetracosane as internal standard and the extracts were transferred into the reactive vials and evaporated with nitrogen gas, derivatized using 20 µl BSTFA (N, O-bis-trimethylsilyltrifluoracetamide) and 20 µl pyridine at 70°C for 40 min. These samples were then analysed with gas chromatography (Richardson et al., 2005).

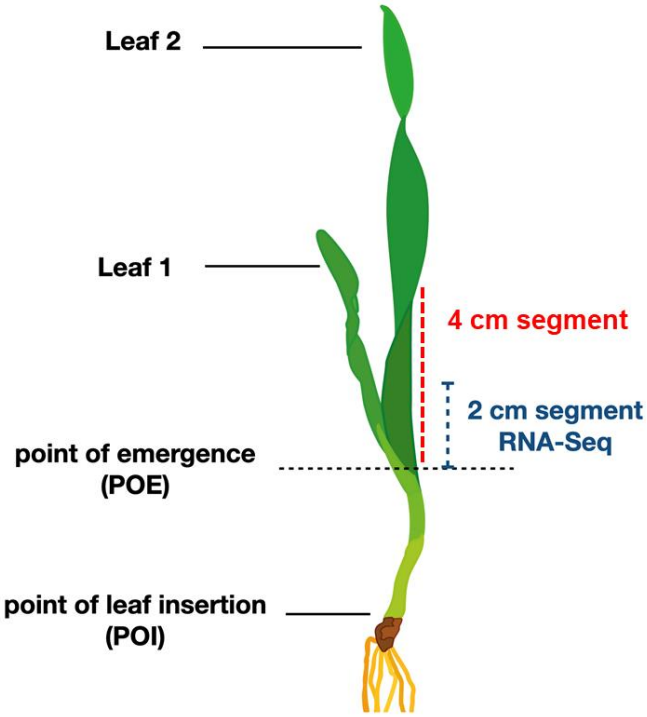

Figure 4 Scheme of barley leaf referring to locations for GC analysis and RNA-sequencing Whole leaf wax and cutin analysis were done separately for leaf 1 and leaf 2 from the point of emergence (POE) region. Since the deposition of wax begins from the POE region of the older leaf, the wax and cutin analysis were also done at the beginning of leaf 2 from POE of leaf 1 (red line). For RNA-Seq analysis of wax and cutin genes, 2 cm segments of leaf 2 (blue line) from POE region were harvested to avoid the overload of the material. POI – Point of leaf insertion (base of the leaf); POE – Point of emergence where the new leaf emerges into the atmosphere.

The leaves used for wax extraction were also used for cutin analysis. They were incubated in the vials containing chloroform: methanol (1:1) at room temperature under continuous shaking for two weeks for lipid extraction. Finally, the leaf samples were dried and stored in a desiccator containing activated silica gel. Before transesterification, the samples were weighed with the analytical balance (Sartorius CPA225D weighing balance) with a resolution of ± 0.01 mg and transesterified at 70ºC for 16 h by adding 2 ml of Boron trifluoride-methanol. After 16 h the sample was cooled and 10 µg/50 mg of dotriacontane was added as an internal standard. The transesterification reaction was stopped by transferring the extract into new vials containing sodium carbonate ($NaHCO_3/H_2O$). The cutin monomers were extracted with 1-2 ml of chloroform. The extract was washed thoroughly with 1.5 ml of HPLC water by vortexing the sample and discarding the water phase. Anhydrous sodium sulphate was used to remove the excess water. Following, the extracts were

transferred to new reactive vials and up concentrated by evaporating under Nitrogen gas at 60ºC until the desired volume is achieved. Later the samples were derivatized with 20 µl BSTFA (N, O-bis-trimethylsilyltrifluoracetamide) and 20 µl pyridine at 70ºC for 40 min. During derivatization, the active hydroxyl groups are replaced with trimethyl ethers, a process of silylation contributing to chemical and thermal stability for the analytes for gas chromatography (GC) (Orata, 2012). Minimum three biological replicates were used for this experiment.

2.9 Analysis by GC-MS and GC-FID

The derivatized samples (approx. 100 µl) were transferred to the autosampler vials and run on gas chromatography. It injects 1 µl of the sample into the DB-1 column of 30-meter-long, 0.32 mm diameter, 0.1 µm poly (dimethylsiloxane) coating.

The quality of the column should be checked before and after running the samples in GC via a standard acid solution containing a mixture of alkane (C_{24}) and three carboxylic acids (C_{29}, C_{30}, C_{31}) in chloroform and derivatization is done as mentioned in 2.8. The acid standard is run on GC-FID with the special temperature profile (**Table 2**). For the detected amount of alkane to the C_{31} carboxylic acid the intensity ratio ≤ 1.3, indicates the column with sufficient quality.

Table 2 Temperature program for acid standard

Program	Temperature rise (ºC/min)	Final temperature (ºC)	Temperature hold (min)
ACID STANDARD		50	1
	40	200	2
	3	310	20

GC-FID (Flame Ionization Detector- Agilent technologies, 6890N Network Gas Chromatography) analyse the samples quantitatively for the concentration of wax/ cutin monomers. It uses hydrogen flame to ionize the samples which are arriving at the detector, releasing free electrons. Proportional to the electrons, signals are produced which are generated in the form of chromatograms. The temperature profile used for GC-FID is given in **Table 3**.

Table 3 Temperature program for GC-FID analysis

Program	Temperature rise (ºC/min)	Final temperature (ºC)	Temperature hold (min)
WAX		50	2
	40	200	2
	3	310	30
CUTIN		50	2
	10	200	1
	3	310	20

GC-MS (Mass Spectrometry- Agilent technologies, 7890B/5977A Series Gas Chromatograph/Mass Selective Detector) analyse the molecules qualitatively to identify the compounds. The molecules of the sample are ionized into fragments. Depending on the mass per charge ratio, the quadrupole mass analyzer identifies the components at the molecular level. Each fragment is identified with the help of Agilent software - GC/MSD Mass Hunter Acquisition with both Mass Hunter and Classic Chem Station Data Analysis and compared to the databases of Prof. Schreiber's laboratory (Department of Ecophysiology, Institute of Cellular and Molecular Botany, Bonn, Germany). The temperature profile used for GC-FID is given in **Table 4**.

Table 4 Temperature program for GC-MS analysis

Program	Temperature rise (ºC/min)	Final temperature (ºC)	Temperature hold (min)
WAX		50	2
	40	200	2
	3	310	30
CUTIN		50	2
	45	200	1
	3	300	15

2.10 RNA isolation

The deposition of cuticular waxes begins from the portion that is enclosed within the sheaths of older leaf and the wax genes are expressed at the commencement of wax deposition (Richardson et al., 2005). For RNA isolation, four 2 cm segments of leaf 2 from the POE region of leaf 1 were pooled as one replicate for enough leaf material and were frozen in liquid nitrogen. Similar to the root transcriptomics done previously, for chemical analysis 4 cm region was used and half of the region for leaf transcriptomics. RNA was isolated with RNeasyPlus Universal Mini Kit (Qiagen, Venlo, the Netherlands) in the same way as described in (Kreszies et al., 2019). Later the RNA quality was analyzed via Nanodrop (Thermo Fischer Scientific, Wilmington, Delaware, USA) and Agilent RNA 6000 Nano Chip (Agilent Technologies, Santa Clara, CA, USA) Bioanalyzer. RNA integrity number was detected at ≥ 7.8 for all samples. Four biological replicates were used for this experiment.

2.11 Processing of raw data

Reads were obtained with an IlluminaHiSeq 4000 sequencer (BGI Tech Solutions, Hong Kong, China). The raw sequencing reads consisting of 100-bp paired-end reads were processed via CLC Genomics Workbench v.10.0.1 (https://www.qiagenbioinformatics.com/) and mapped to the barley reference genome. The raw reads were processed in the same way as described by (Kreszies et al., 2019; Osthoff et al., 2019). Low-quality reads were trimmed and removed from the dataset and reads with > 40bp were mapped to the barley reference genome Hv_IBSC_PGSB_v2 (Mascher et al., 2017) allowing large gaps of up to 50 kb to span introns. Reads that matched with a length ≥ 80% and identity ≥ 90% to the reference genome were considered as mapped. Stacked reads, i.e. read pairs having identical 5’ coordinates, orientation and length were merged and removed from the dataset. Consequently, remaining reads were mapped to the set of high-confidence gene models H v_IBSC_PGS_v2.36 (Mascher et al., 2017). Only reads that matched with length ≥ 90% and identity ≥ 90% to the transcripts of the high confidence gene models were considered as mapped. Reads with more than one hit were removed from the read counting.

To meet the assumptions of the linear model, the read counts were normalized by the sequencing depth and $\log_2$-transformed. The mean-variance relationship was

estimated and used to assign precision weights to adjust the heteroscedasticity (Law et al., 2014; Ritchie et al., 2015). Bayer's approach was applied to estimate the variability over all genes and to shrink the variances towards a common value (Smyth, 2004). A linear model was fitted to access the variation in gene expression between the treatments. The contrast.fit function of R package *limma* was used to compute the pairwise comparisons between the treatments. The calculated p-values of the performed pairwise t-tests were corrected by adjusting the false discovery rate (FDR) to ≤ 5%.

2.12 Statistical analysis

Statistical analysis was done with ORIGIN PRO 9. Statistical differences were tested between the treatments at a significance level of 5%. Hypothesis testing (two-sample t-test) was done for root and shoot lengths. One-way analysis of variance (ANOVA) with Fisher's LSD test ($p<0.05$) was used for all physiological and chemical analysis.

3 Results

3.1 Effect of osmotic stress on the shoot and root development

Elongation of root and shoot length was measured during the whole growth period of 12 days (**Figure 5**).

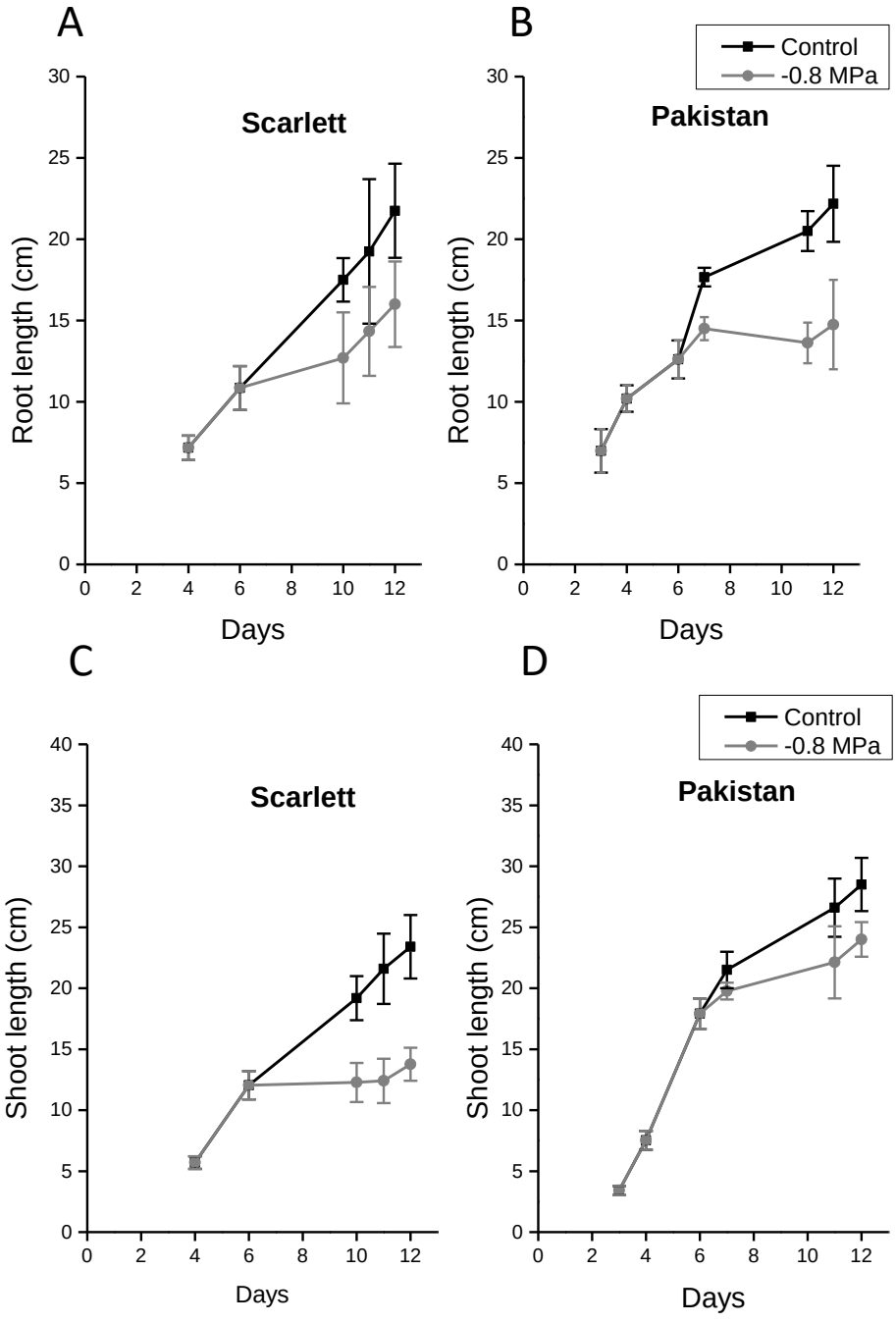

Figure 5 Effect of osmotic stress on root and shoot development Elongation of the root (A, B) and shoot (C, D) was measured over the 12-d growth period and the application of PEG8000 affected the root and shoot elongation.

Reduction in water potential affects the growth of root and shoot development from the beginning of stress application. The maximal root length was affected by 26% for cultivar Scarlett and 33.5% for wild accession Pakistan. The maximal shoot length was affected by 41% for cultivar Scarlett and 15% for wild accession Pakistan.

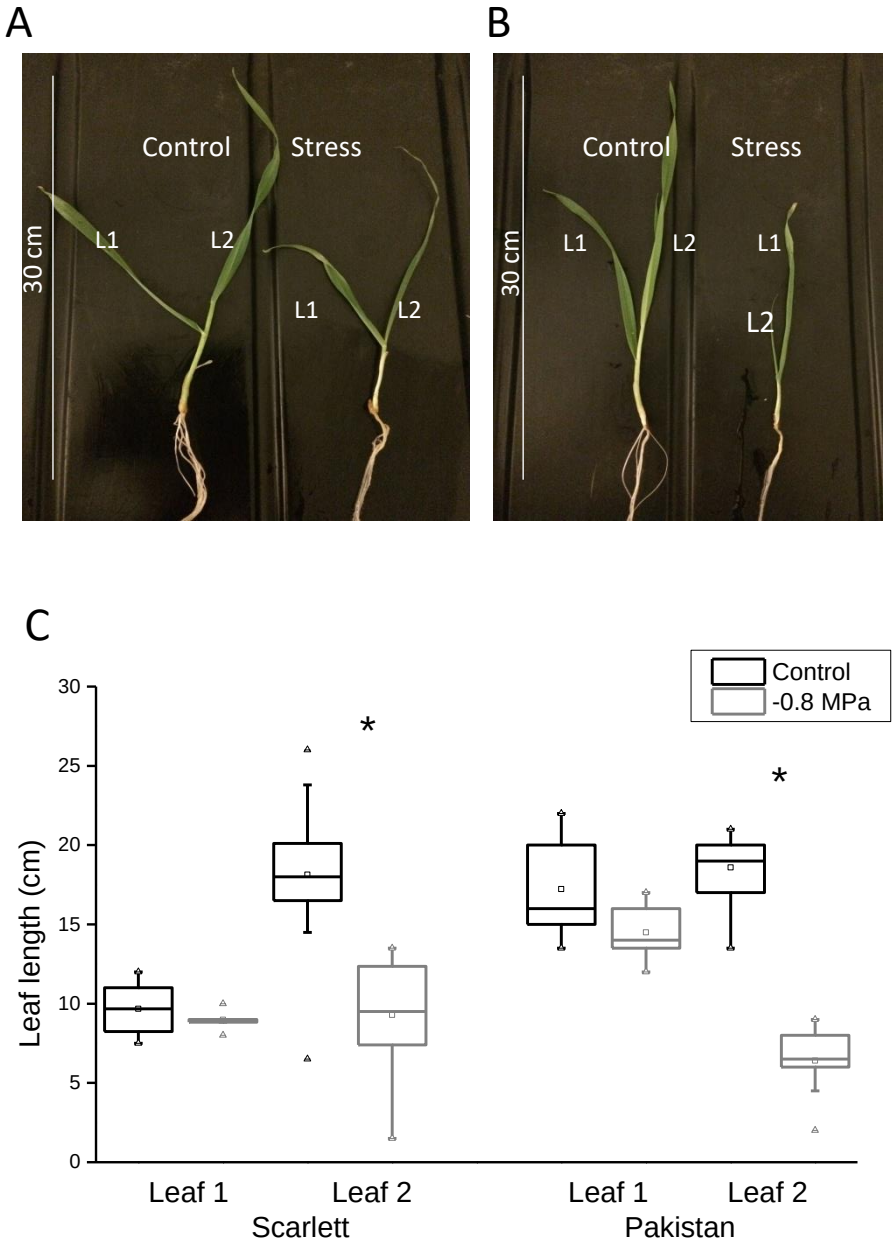

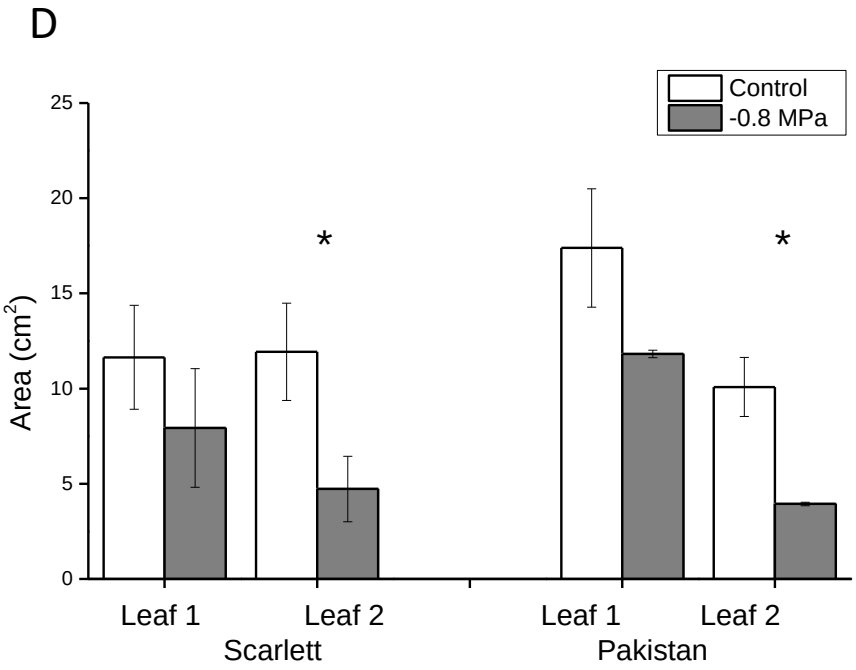

Figure 6 Effect of osmotic stress on barley leaves (a,b) 12-d old barley leaves with and without the application of PEG8000 (A) cultivar Scarlett and (B) wild type Pakistan. (C) Leaf lengths of 12-d old barley plants were measured for both cultivar Scarlett and wild accession Pakistan and plotted as box plots with a minimum of 10 replicates. Outliers are plotted as whiskers. Mean values are denoted by the small square inside the box. (D) The area of the 12-d old leaves was scanned and measured. Bars indicate means with a minimum of 10 replicates and their corresponding standard deviation. The asterisk represents a significant difference between the control and stress leaf. Significant differences between means are at a significance level of 0.05 tested in one-way ANOVA (Fisher's LSD test).

Twelve-day-old hydroponically grown barley plants have two leaves and the application of PEG8000 especially affects the development of leaf 2 (**Figure 6** A, B). Osmotic stress leads to inhibition of leaf growth. While there was no significant effect on leaf 1, leaf 2 growth was inhibited by 49% for cultivar Scarlett and 66% for wild accession Pakistan. This suppression in leaf length is attributed with a reduced area of leaf 2 significantly for both the investigated cultivars (**Figure 6** C, D).

3.2 Cell length and stomatal index

Lengths of the cells in-between the stomata of leaf 1 and leaf 2 of both cultivars were measured from the Collodium imprints. Application of PEG inhibits the cell length of leaf 1 by 9% for cultivar Scarlett and 16% for wild accession Pakistan while the cell length of leaf 2 was repressed by 51% for cultivar Scarlett and 35% for wild accession Pakistan (**Figure 7**and **Figure 8**A).

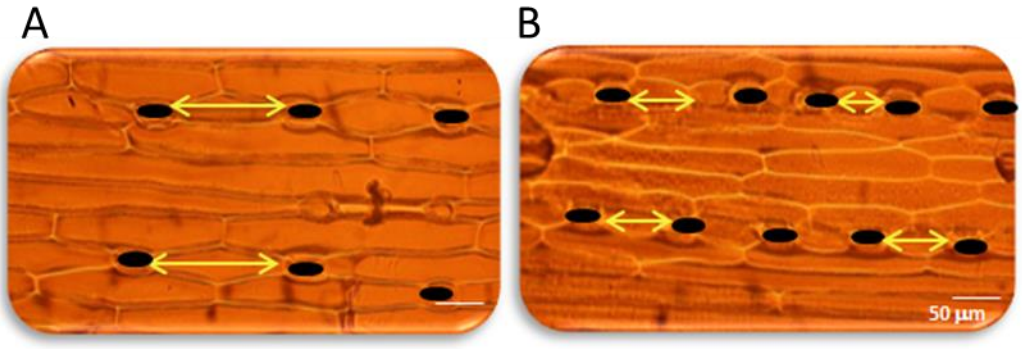

Figure 7 Microscopic observation for cell elongation by barley leaf 2 imprints The cell elongation was reduced significantly as a result of osmotic stress. (A) The control leaf imprints (B) stress leaf imprints (figure given for cultivar Scarlett). Stomata are highlighted with the black circle. Images were taken at the scale bar 50 µm.

Stomatal Index was determined to investigate the change in the distribution of the stomata (S) in the epidermal cells (P). The tendency of stomatal distribution was similar in both the leaves for both the cultivars (**Figure 8**B).

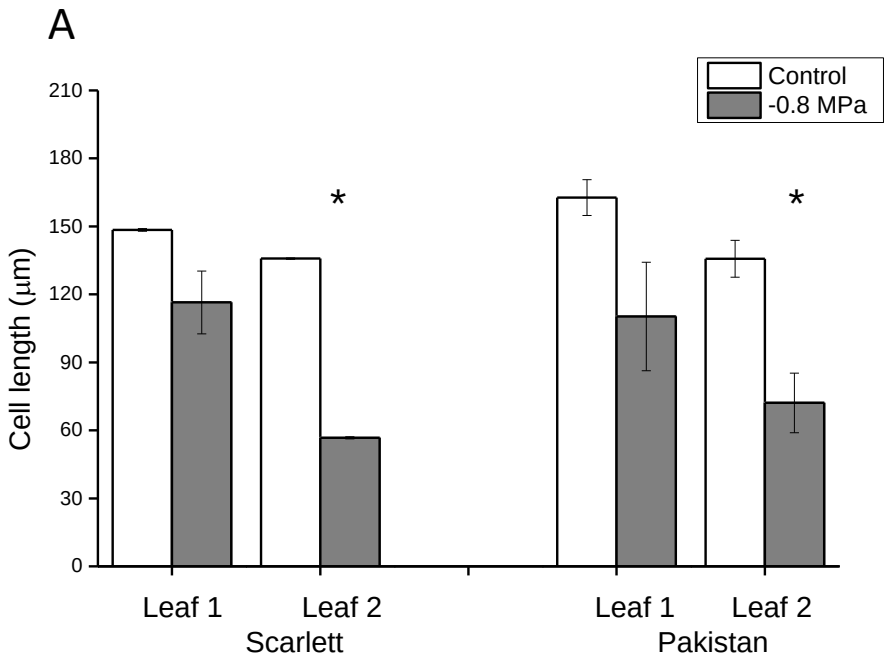

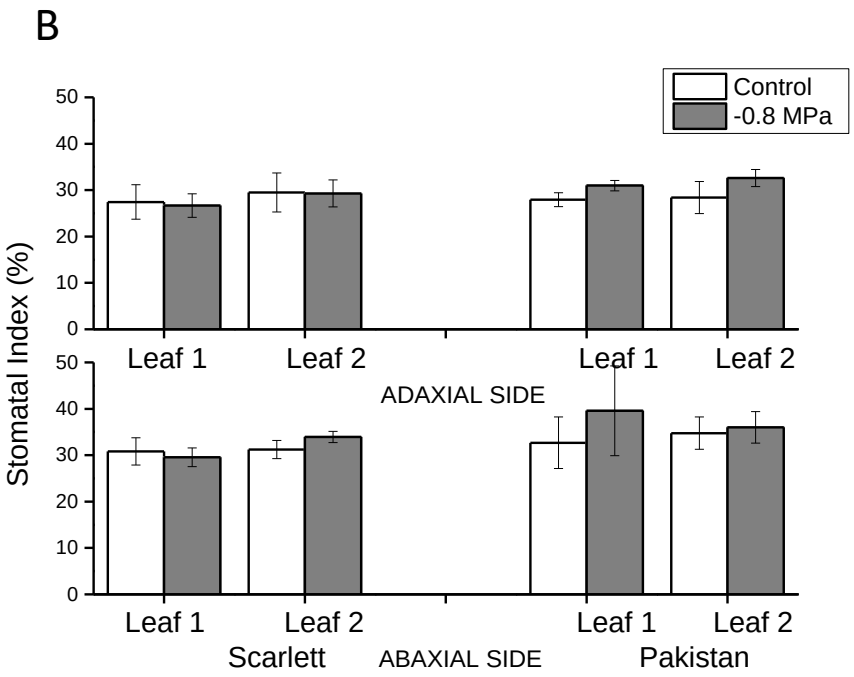

Figure 8 Effect of osmotic stress on cell lengths (A) The length of the cells in between the stomata was measured for both leaf 1 and leaf 2. (B) The stomatal distribution for both the leaves on the abaxial and adaxial side of the leaf was calculated by stomatal index. Bars indicate means of a minimum of three replicates with the corresponding standard deviation. With a minimum of 10 replicates for cell length, the significant differences between means are at a significance level of 0.05 tested in one-way ANOVA (Fisher's LSD test).

3.3 Stomatal transpiration

Stomatal conductance was measured immediately after the application of PEG8000 and the transpiration decreased significantly 3-fold in 30 min after reducing the water potential. After 30 min the stomatal conductance remains steady for the stressed plants over the next days. Comparing the genotypes, the cultivar Scarlett showed a slightly lower variability of the conductance compared to the wild accession Pakistan.

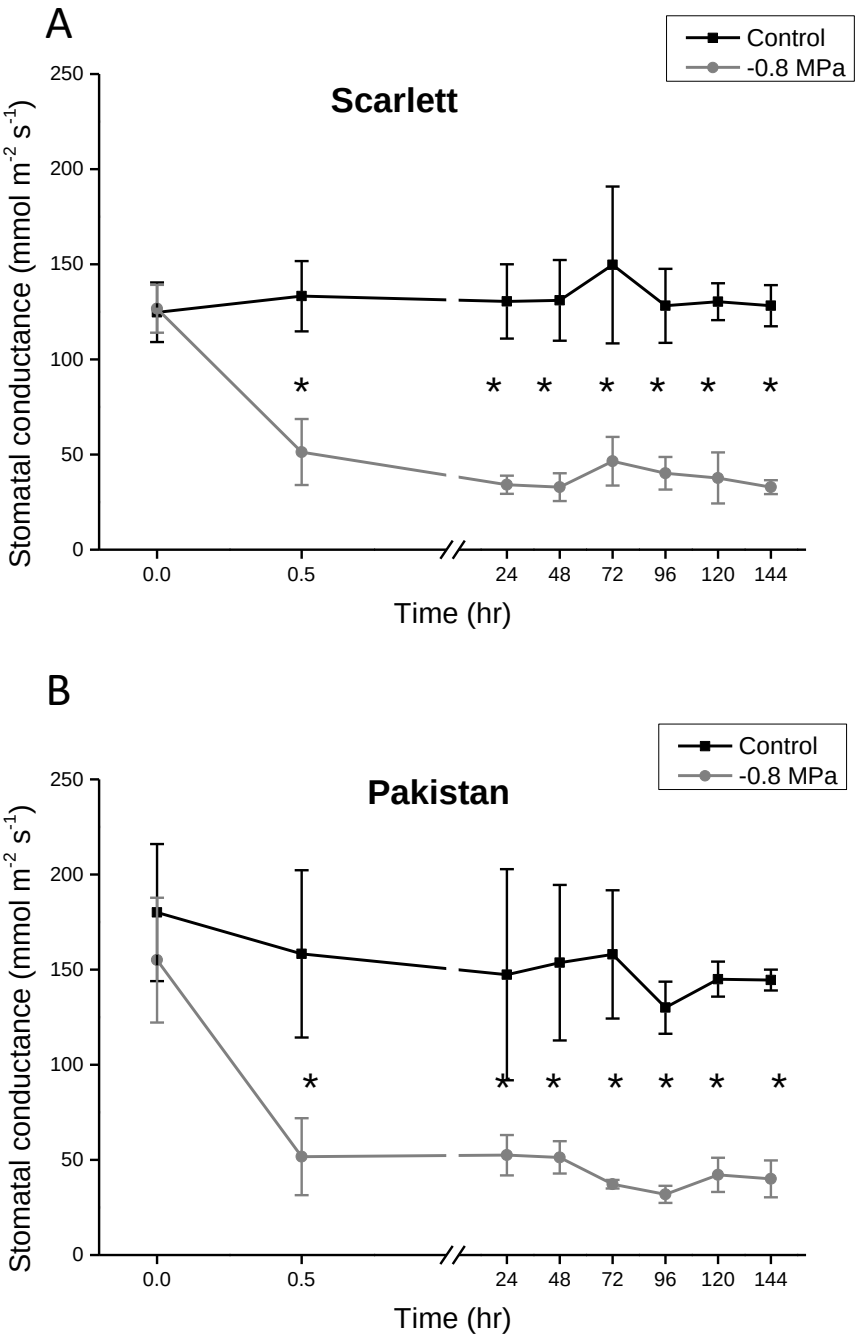

Figure 9 Effect of osmotic stress on stomatal transpiration on the adaxial side of the leaf Adaxial leaf transpiration for (A) cultivar Scarlett and (B) wild accession Pakistan. Black symbols indicate the transpiration of control plants and grey symbols indicate the transpiration of the osmotically stressed plants. The asterisk represents a significant difference between the control and stress leaf. With a minimum of three replicates, the significant differences between means are at a significance level of 0.05 tested in one-way ANOVA (Fisher's LSD test).

Adaxial leaf transpiration dropped from 124.78 ± 36.06 mmol m^{-2} s^{-1} to 51.29 ± 17.34 mmol m^{-2} s^{-1} for cultivar Scarlett (**Figure 9**A) and 180 ± 36.06 mmol m^{-2} s^{-1} to 51.67 ± 20.21 mmol m^{-2} s^{-1} for wild accession Pakistan (**Figure 9**B) while abaxial leaf

transpiration was 10-fold lesser compared to the adaxial side irrespective of the cultivar (**Supplementary Figure 1**).

3.4 Residual transpiration from detached leaves

Residual transpiration for detached barley leaves was calculated based on the water loss over time. The transpirational water loss stayed constant about 1 h after the leaf detachment for both cultivar Scarlett and wild accession Pakistan. The initial transpiration loss is contributed by the stomatal opening and after 1 h when most of the stomata being closed, transpiration is controlled by cuticles and few unclosed stomata (**Figure 10A**). The mean permeance between control Scarlett (7.49 E^{-10} ± 1.62 E^{-10}) and control Pakistan (5.15 E^{-10} ± 9.45 E^{-11}) was statistically significant. Likewise, the mean permeance between the stress Scarlett (9.41 E^{-10} ± 1.91 E^{-10}) and stress Pakistan (5.51 E^{-10} ± 1.11 E^{-10}) was also statistically significant from each other. However, between the treatments, they were statistically insignificant (**Figure 10B; Supplementary Figure 2**).

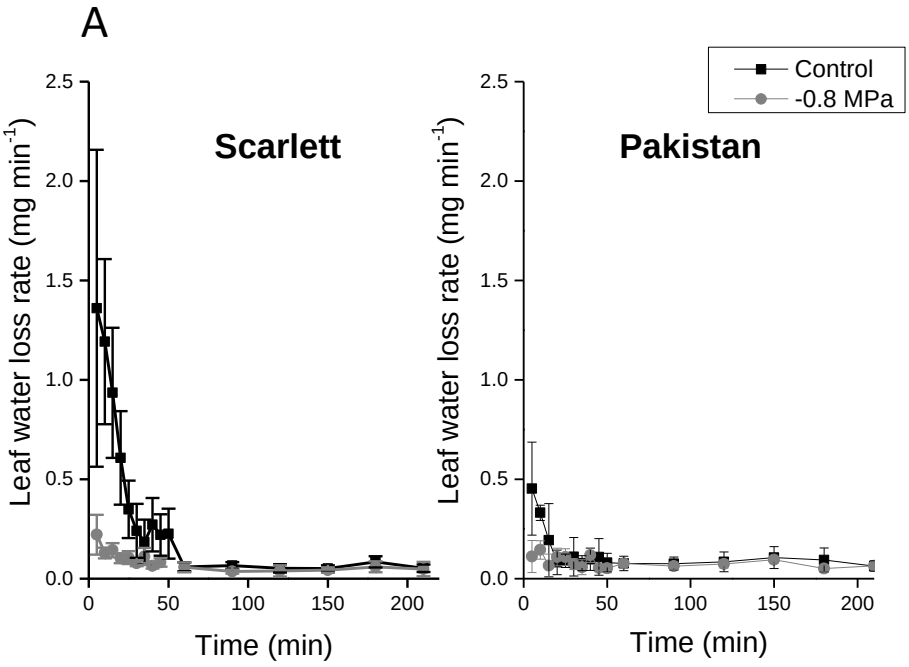

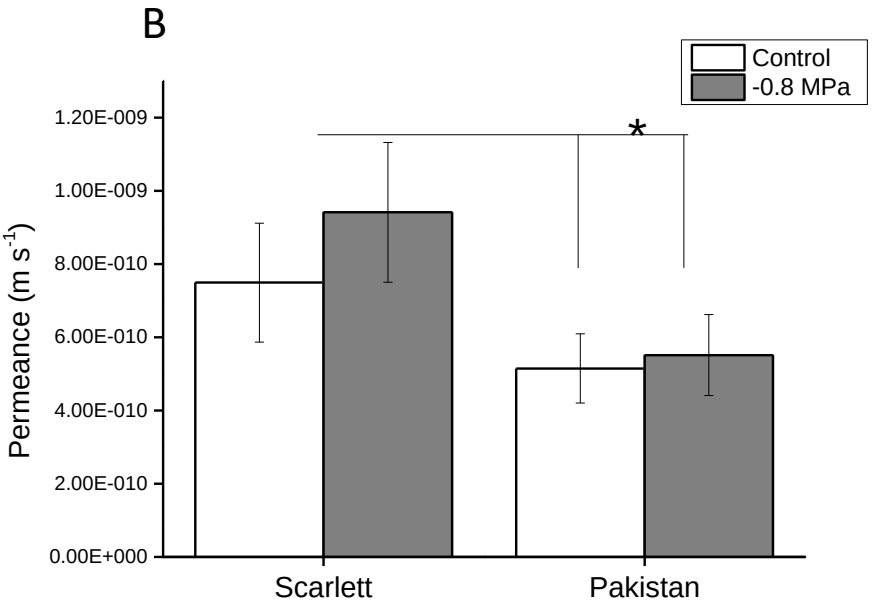

Figure 10 Residual transpiration of detached leaves (A) Water loss over time was measured to calculate the residual leaf transpiration of barley leaves. Black square symbol indicates the effect of control plants and the grey circle symbol indicates the effect of stressed plants. (B) Total minimum leaf conductance of both cultivars. Wild accession Pakistan leaf conductance is lower compared to Scarlett. The asterisk represents a significant difference. With a minimum of four replicates, the significant differences between means are at a significance level of 0.05 tested in one-way ANOVA (Fisher's LSD test).

3.5 Light response curve

Measurements for the light curve were immediately recorded after the application of PEG8000. Data obtained from the light curve shows the quantum yield (II), which is the photochemical quantum yield of photosystem II,(Y(II)), decreases gradually with increasing Photosynthetic active radiation (PAR) and they were almost reduced by 60% at 820 µmol m^{-2} s^{-1} (**Figure 11**A). The increase in the Y(II) in the beginning was due to the better optimization of photons used in photochemistry. While at a higher light intensity, the proton gradient was slowed down resulting in minimizing energy-dependent quenching. Electron Transfer Rate (ETR) derived from Y(II) and PAR, increases with increasing light intensity (**Figure 11**B). There was no significant difference between Scarlett and Pakistan.

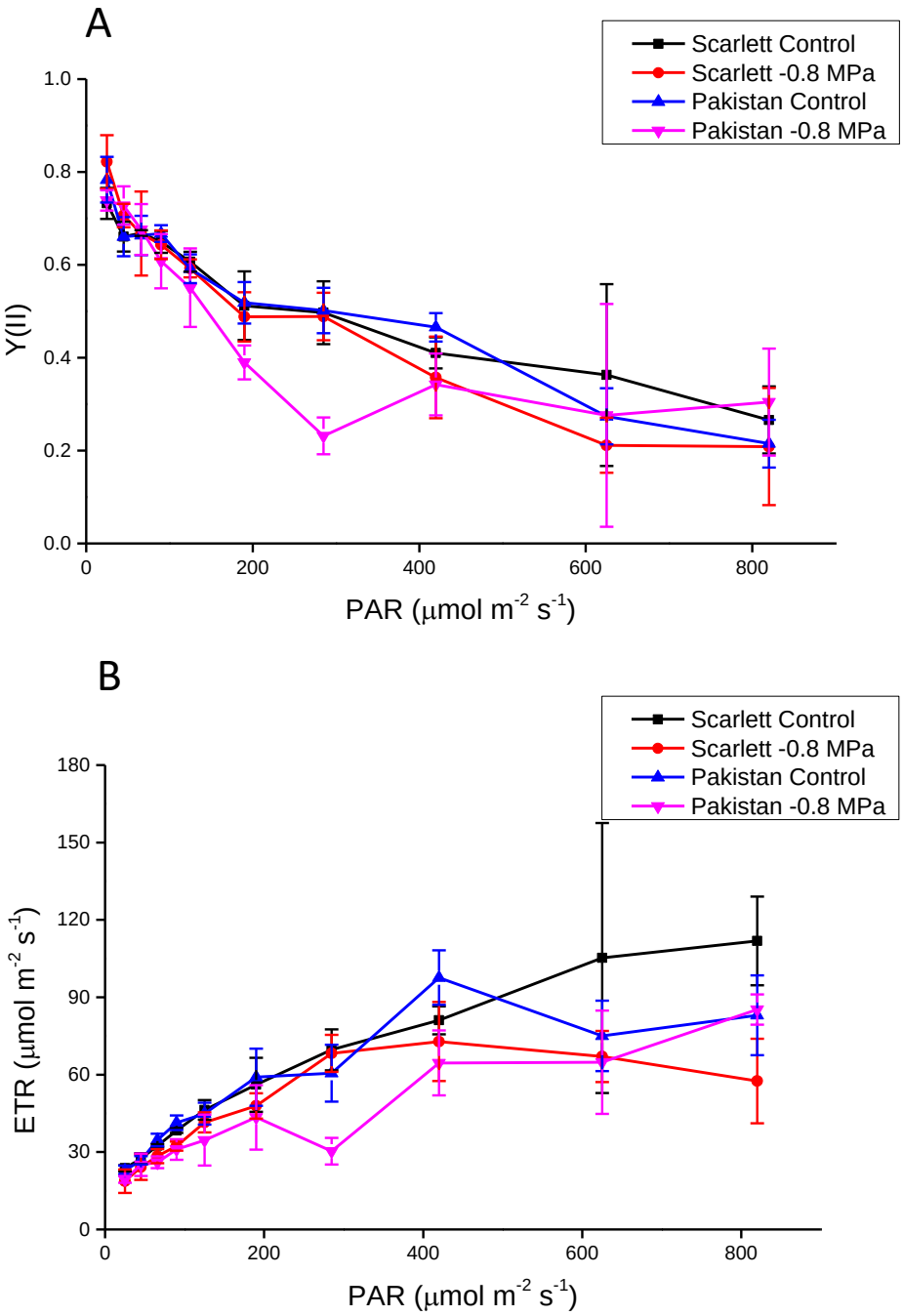

Figure 11 Light curves of quantum yield (II) and electron transport in barley leaves (A) Effect of high-light treatment on the quantum yield of photosystem II (Y(II)) for cultivar Scarlett and wild accession Pakistan (B) the effect of high-light treatment on electron transfer rate (ETR) for cultivar Scarlett and wild accession Pakistan. With a minimum of four replicates, no significant differences were observed between means at a significance level of 0.05 tested in one-way ANOVA (Fisher's LSD test).

3.6 Estimation of Proline concentration

Proline accumulation under osmotic stress plants was compared with the control plants of leaf 1 and leaf 2 together. Proline content was enhanced significantly from

105.37 ± 46 µg g^{-1} to 206.60 ± 125.50 µg g^{-1} for cultivar Scarlett and from 83.65 ± 46 µg g^{-1} to 128.69 ± 56.07 µg g^{-1} for wild accession Pakistan (**Figure 12**).

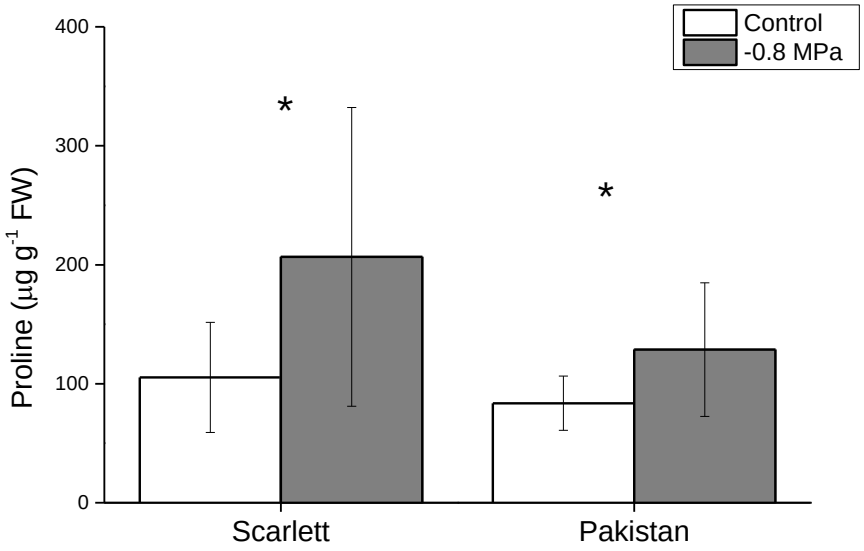

Figure 12 Estimation of proline concentration Proline accumulation under osmotically stressed plants was measured and compared with the control plants. The asterisk represents a significant difference in proline accumulation. With a minimum of eight replicates, the significant differences between means are at a significance level of 0.05 tested in one-way ANOVA (Fisher's LSD test). Asterisk indicates a significant difference between the treatment.

3.7 Scanning Electron Microscopy

Investigation of leaf wax structures was done with SEM since the wax composition influences the wax morphology. Wax crystals were oriented perpendicular towards the leaf surface which was linear and plate-shaped for both Scarlett (**Figure 13** A-D) and Pakistan (**Figure 13** E-H). There was no difference observed between the control leaf SEM pictures (**Figure 13** A, C, E, G) and mostly the wax crystals were oriented singularly. More densely and interconnected platelets were noted for the stress-treated leaves (**Figure 13** B, D, F, H) indicating more deposition of wax.

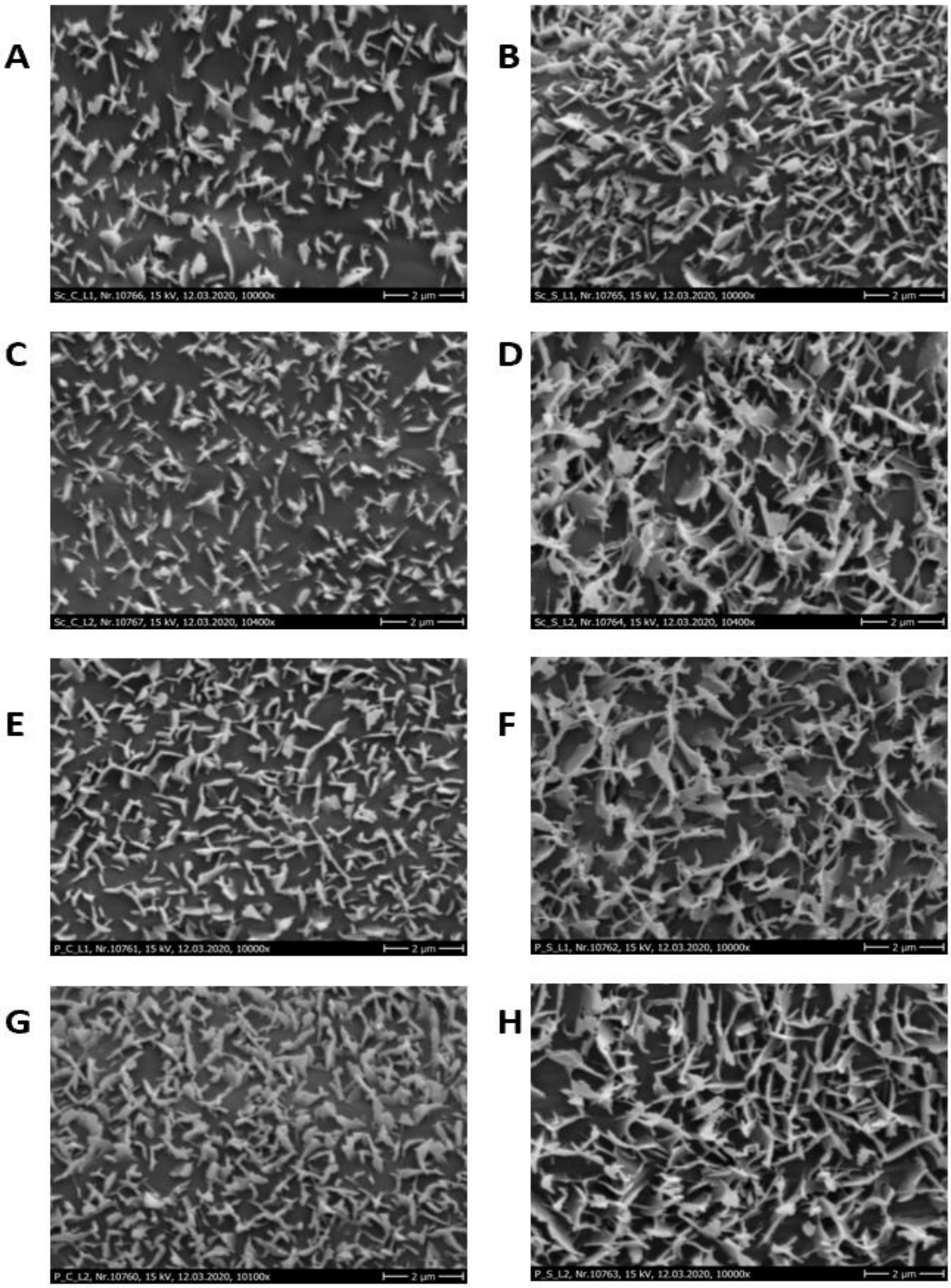

Figure 13 Investigations of leaf morphology by scanning electron microscope 12-d old plants were harvested and approximately 2.5 cm of central leaf portion was investigated for leaf wax structures with SEM. A, C – Scarlett control leaf 1 & leaf 2; B, D – Scarlett stress leaf 1 & leaf 2; E, G – Pakistan control leaf 1 & leaf 2; F, H – Pakistan stress leaf 1 & leaf 2.

3.8 Chemical analysis of wax

For chemical analysis of wax, whole-leaf 1 and leaf 2 were analysed separately. Cuticular waxes were composed of four main monomer classes: fatty acids, alcohols, aldehydes and esters. A similar deposition trend of wax was observed between the cultivar Scarlett and wild accession Pakistan. Wax analysis of whole leaf 1 yielded the same amounts between the control and stressed plants. In contrast, for leaf 2, a significant reduction in total wax coverage of the whole leaf was observed (**Figure 14**A). The distribution of amounts of the whole leaf in different classes is shown in (**Figure 14**B). This reduction in wax coverage was attributed by the decrease in the leaf area (**Figure 6**D).

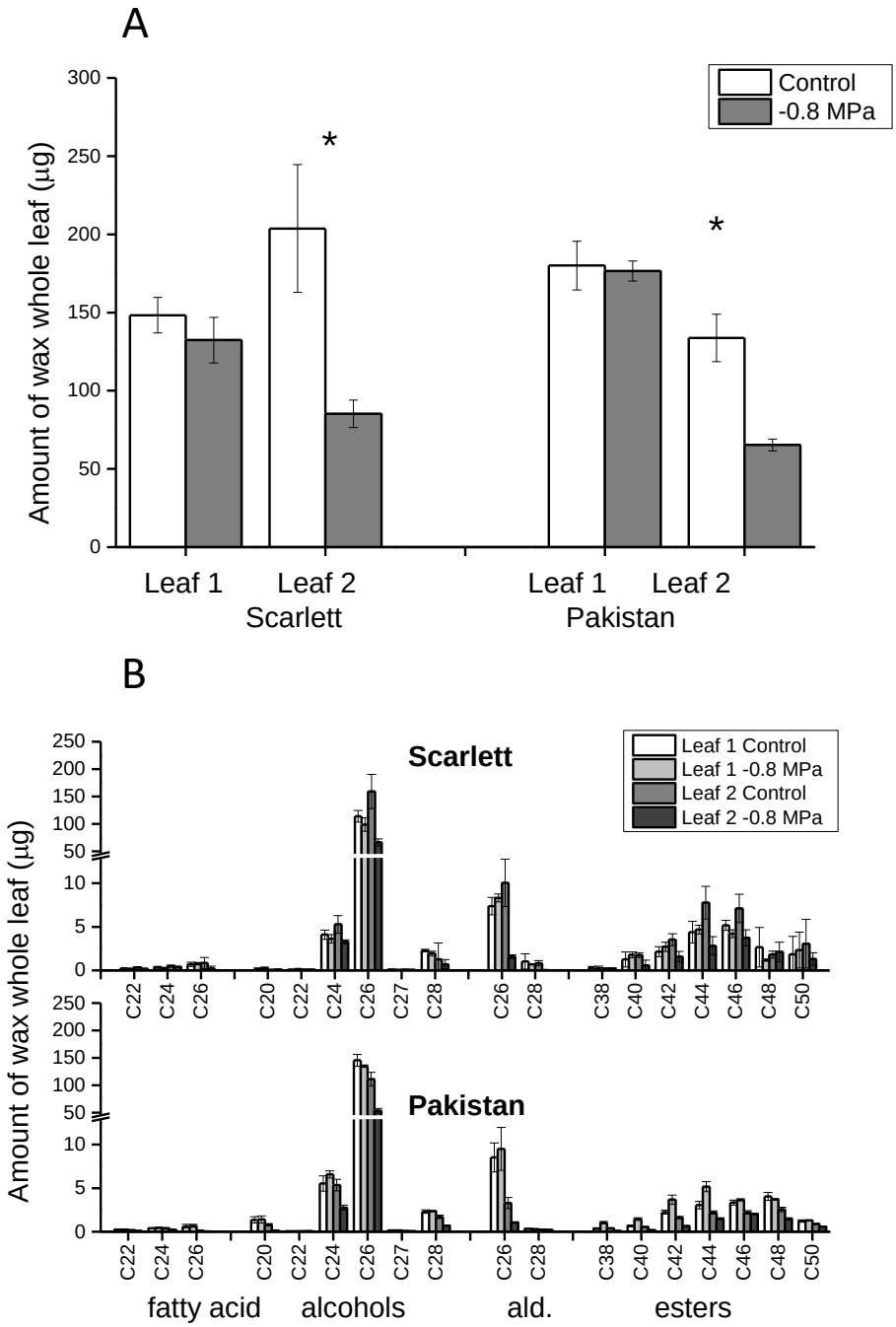

Figure 14 Wax amounts expressed as whole leaf Wax extracted from whole leaf 1 and leaf 2 of cultivar Scarlett and wild accession Pakistan is represented. (A) The total amount of wax (B) cuticular waxes were composed of four main monomer classes: fatty acids, alcohols, aldehydes and esters with chain length ranging from C_{20} to C_{50}. Bars indicate means with the corresponding standard deviation. The asterisk represents a significant difference between the control and stress leaf. With three replicates, the significant differences between means are at a significance level of 0.05 tested in one-way ANOVA (Fisher's LSD test).

Expressing the wax amounts with respect to the area of the leaf, a significant increase of nearly 40% under osmotic stress for leaf 1 was observed which ranged from 11.58 ± 1.79 µg/cm^2 to 16.09 ± 0.74 µg/cm^2 for cultivar Scarlett and

10.51 ±1.47 μg/cm^2 to 14.94 ± 0.73 μg/cm^2 for wild accession Pakistan (**Figure 15**A). An increase of 20% wax coverage was observed in leaf 2 for cultivar Scarlett ranging from 15.88 ± 1.41 μg/cm^2 to 19.05 ± 3.55 μg/cm^2 and a significant increase of 32% for wild accession Pakistan from 12.36 ± 1.69 μg/cm^2 to 16.32 ± 0.93 μg/cm^2 under osmotic stress.

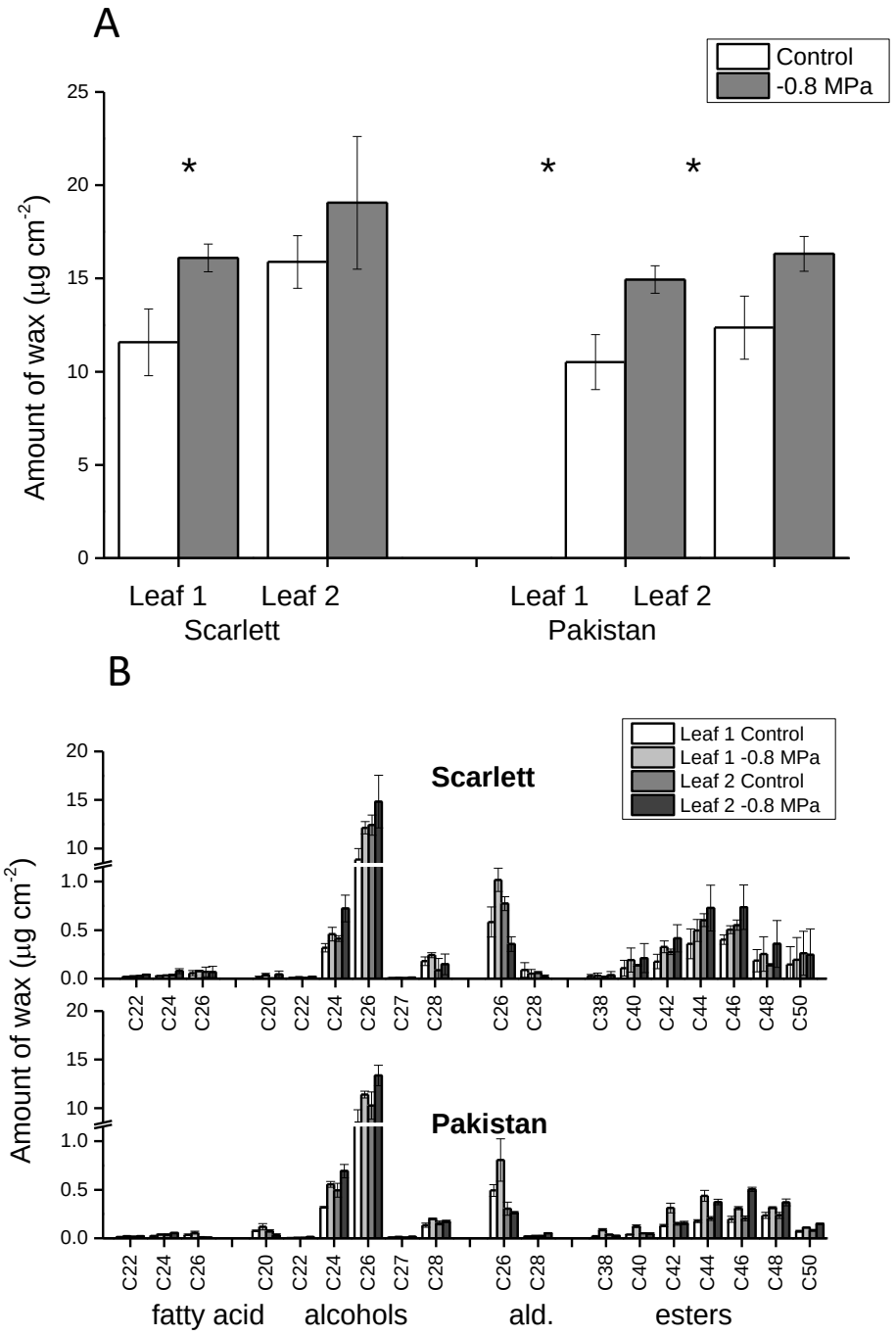

Figure 15 Wax amounts expressed with the area as a reference type Wax extracted from whole leaf 1 and leaf 2 of cultivar Scarlett and wild accession Pakistan is represented with the area as a reference type. (A) The total amount of wax (B) cuticular waxes were composed of four main monomer classes: fatty acids, alcohols, aldehydes and esters with chain length ranging from C_{20} to C_{50}. Bars

indicate means with the corresponding standard deviation. The asterisk represents a significant difference between the control and stress leaf. With three replicates, the significant differences between means are at a significance level of 0.05 tested in one-way ANOVA (Fisher's LSD test).

The carbon chain lengths varied amongst C_{20} to C_{50} monomers (**Figure 15**B). Alcohols ranged from C_{20} to C_{28} with C_{26} being the most abundant and contributing to about 85% of total cuticular wax coverage. Aldehyde chain lengths were made up of C_{26} and C_{28} carbon lengths with C_{26} being maximum. Fatty acid chain lengths were made up of C_{22}, C_{24}, C_{26}, with all three carbon lengths composing the same amounts. The longer chain lengths were made up of esters comprising of C_{38} to C_{50} carbon chains.

3.9 Chemical analysis of cutin

The leaves used for wax analysis were subsequently used for cutin extraction as described in materials (2.8). Similar to the wax deposition pattern, the cutin deposition pattern was the same between the cultivars. Approximately 10% decrease in the cutin amount was observed on whole leaf 1 of both the cultivars (**Figure 16**A). This reduction in cutin coverage was attributed by the decrease in the leaf area (**Figure 6**D). Contradictorily, the cutin amount in leaf 2 of the control and stress plants averaged the same despite the decrease in the leaf area (**Figure 16**A). The distribution of cutin amounts of the whole leaf in different classes is shown in (**Figure 16**B).

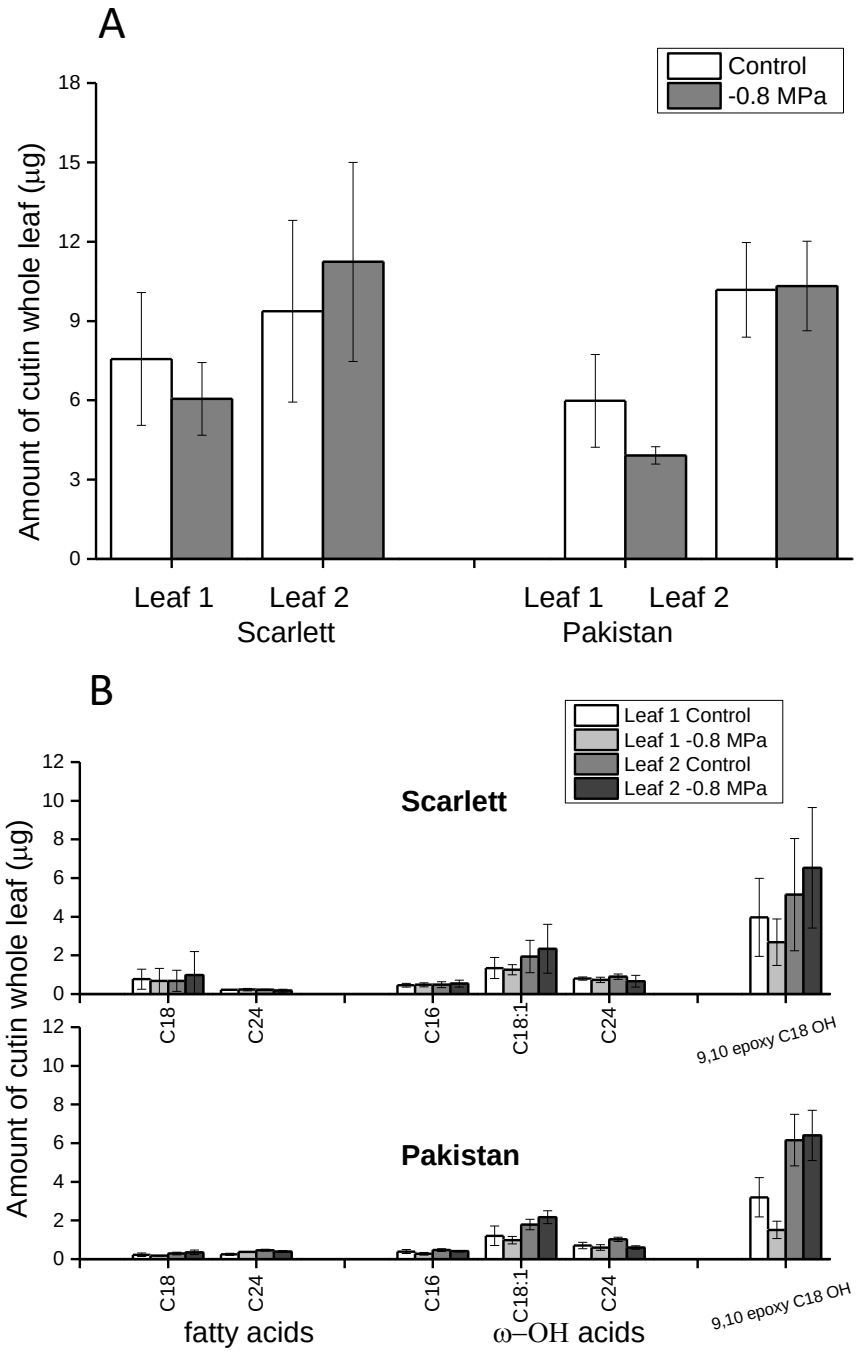

Figure 16 Cutin amounts expressed as whole leaf Cutin extracted from whole leaf 1 and leaf 2 of cultivar Scarlett and wild accession Pakistan is represented. (A) The total amount of cutin (B) cuticular waxes were composed of three main monomer classes: fatty acids, ω-hydroxy acids (OH) and 9,10 epoxy -18 hydroxy acid with chain length ranging from C_{18} to C_{24}. Bars indicate means with the corresponding standard deviation. The asterisk represents a significant difference between the control and stress leaf. With three replicates no significant differences were observed between means at a significance level of 0.05 tested in one-way ANOVA (Fisher's LSD test).

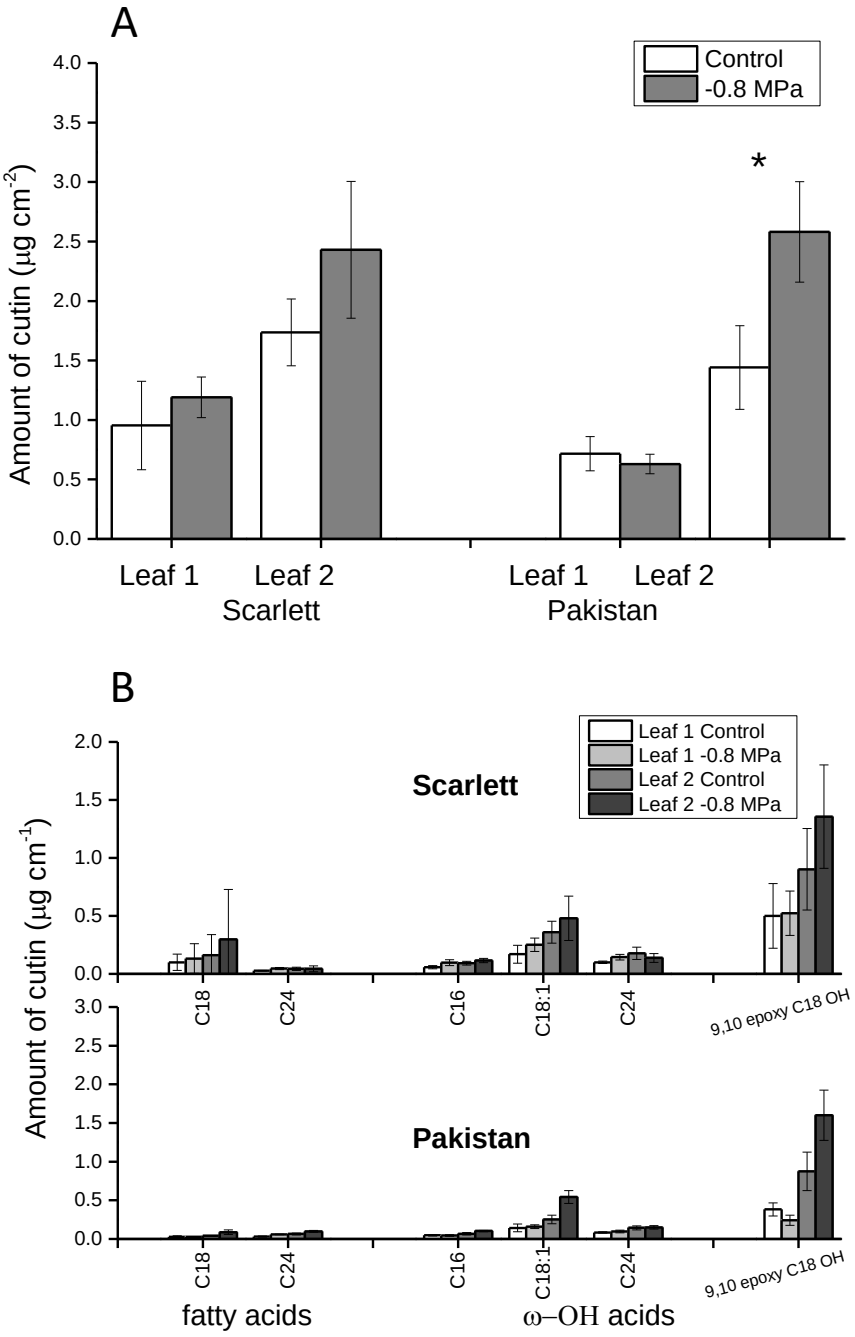

Figure 17 Cutin amounts expressed with the area as a reference type Cutin extracted from whole leaf 1 and leaf 2 of cultivar Scarlett and wild accession Pakistan is represented with the area as a reference type. (A) The total amount of cutin (B) cuticular waxes were composed of three main monomer classes: fatty acids, ω-hydroxy acids (OH) and 9,10 epoxy -18 hydroxy acid with chain length ranging from C_{18} to C_{24}. Bars indicate means with the corresponding standard deviation. With three replicates, the significant differences between means are at a significance level of 0.05 tested in one-way ANOVA (Fisher's LSD test).

Expressing the cutin coverage with the area as a reference type, an increase of 25% from 0.95 ± 0.37 μg/cm^2 to 1.19 ± 0.17 μg/cm^2 for leaf 1 of cultivar Scarlett and 12% decrease for wild accession Pakistan from 0.72 ± 0.14 μg/cm^2 to 0.63 ± 0.08 μg/cm^2 under osmotic stress was observed (**Figure 17**A). In leaf 2 an increase of 40% and

80% of cutin coverage was detected under osmotic stress for cultivar Scarlett and wild accession Pakistan. Cutin was composed mainly of three different substance classes: fatty acids, ω-hydroxy acids and 9(10)-epoxy-18-hydroxy-stearic acid. Fatty acids are made of C_{18} and C_{24} chain lengths, while ω-hydroxy acids are made up of C_{16}, $C_{18:1}$ and C_{24} chain lengths (**Figure 17**B).

3.10 Wax profile of different segments of leaf 2

Along with the gene expression, the wax profile of different segments of leaf 2 from POE of cultivar Scarlett was analyzed as described in methods (2.8).

The GC-FID analysis showed that the wax deposition increased from segment ‘a’ to ‘b’ and stayed stable over the segments ‘b’ for both control and stress treatment (**Figure 18**). Osmotically stressed leaves deposited more wax, mainly the principal compound hexacosanol over the segment ‘c’. Variability in chain lengths differed in-between segment ‘a’ to other segments of the leaf of both control and stress leaves (**Figure 19**).

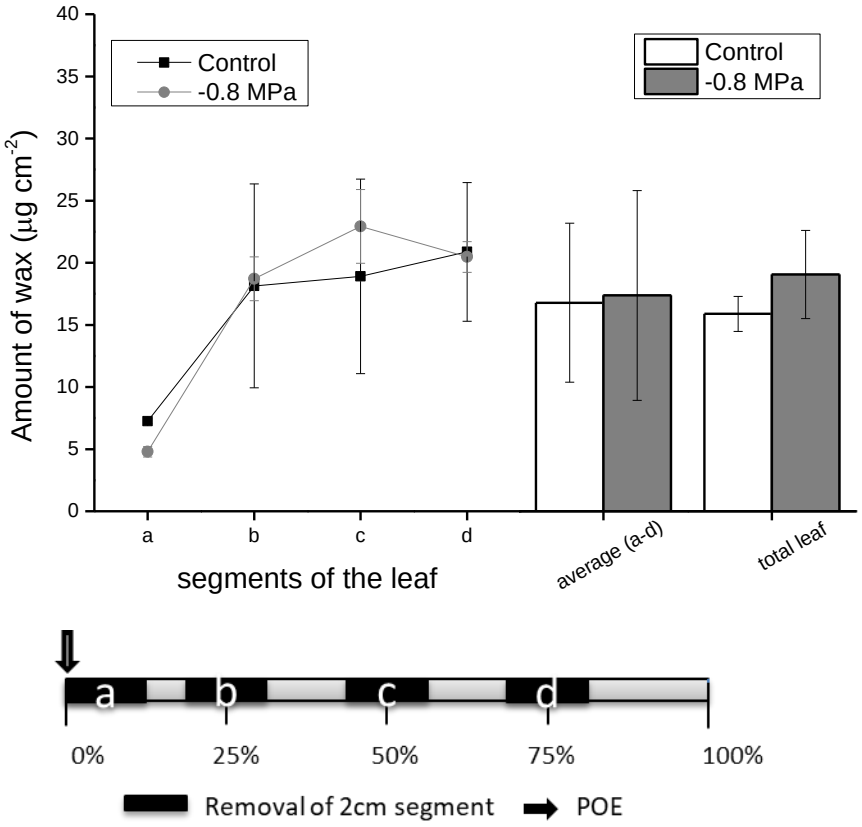

Figure 18 Wax profile of different segments Wax analysis of leaf 2 from POE of cultivar Scarlett increased linearly from segment ‘a’ and stayed constant over the leaf blade. Segment ‘a’ is the region

from POE and segments ‘b-d’ regions along the leaf blade. Bars indicate means with the corresponding standard deviation. With three replicates, no significant differences were observed between means at a significance level of 0.05 tested in one-way ANOVA (Fisher’s LSD test).

From GC-MS analysis, it was identified that some chain lengths including C_{28} aldehyde, $C_{38,\ 40,\ 50}$ esters were absent in segment ‘a’, for both treatments and particularly C_{28} aldehyde was not detected in segments ‘a – c’ under osmotic stress.

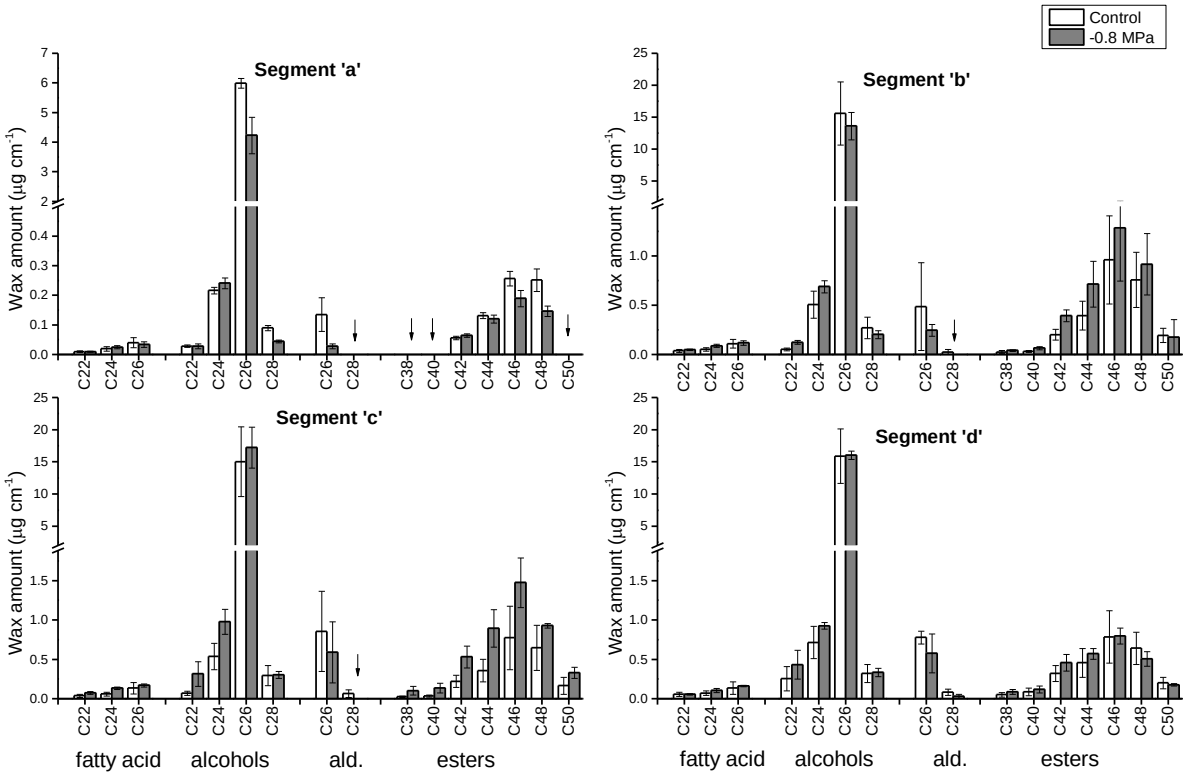

Figure 19 Chain length distribution over different segments Variability in chain lengths differed in-between segment ‘a’ and other segments of the leaf of both control and stress leaf. Bars indicate means with the corresponding standard deviation. With three replicates, no significant differences were observed between means at a significance level of 0.05 tested in one-way ANOVA (Fisher’s LSD test).

3.11 Transcriptomics analysis

Together with leaf transcriptomics, the 4 cm region of leaf 2 from POE was analyzed for wax and cutin amounts. As an effect of osmotic stress, an increase of 35% and 56% of wax amounts for cultivar Scarlett and wild accession Pakistan was observed. Similarly, the cutin amounts increased 91% for Scarlett and 214% for Pakistan. Contrary to chemical analysis half of the region was used for transcriptomics to identify the gene expression changes due to osmotic stress. Differentially expressed genes (DEGs) were computed in three pairwise contrasts between the treatments. At an FDR

≤ 5%, the number of DEGs varied between the treatments and is depicted as volcano plots (**Figure 20**). For cultivar Scarlett, there were 2411 unique up-regulated genes and 1284 unique down-regulated genes. For wild accession Pakistan, there were 380 unique up-regulated genes and 169 unique down-regulated genes. Among the upregulated DEGs lipoxygenase and defense responsive related genes were highly enriched for both genotypes. Cross-comparison between the number of DEGs in between the control and stress treatment and comparison in between the genotypes is depicted as the Venn diagram (**Figure 21**).

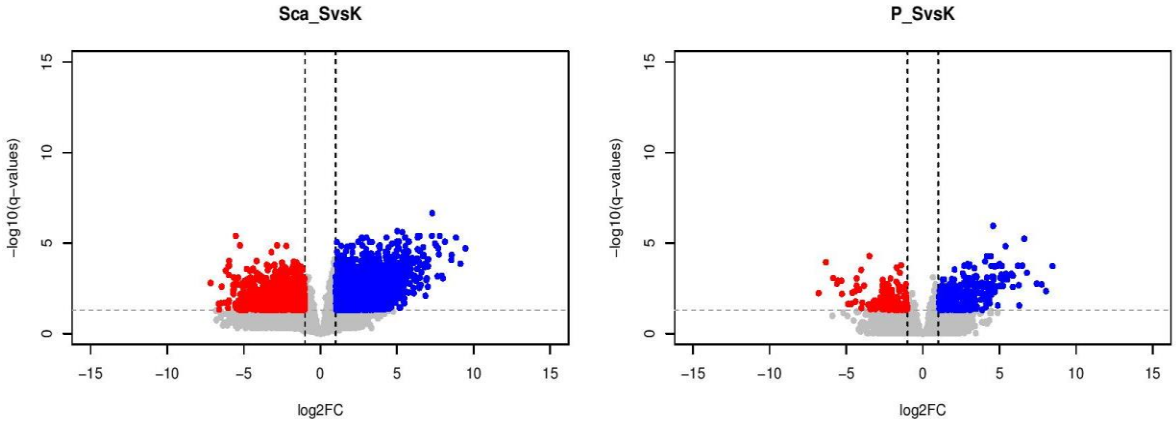

Figure 20 Overview of differentially expressed genes (DEGs) by volcano plots Volcano plots depict DEGs for in-between the control and stress leaves for cultivar Scarlett and wild accession Pakistan. Up-regulated DEGs are indicated by blue dots, down-regulated DEGs are indicated by red dots. DEGs not exceeding the threshold of |log2FC| >1 and FDR ≤1% are indicated in grey.

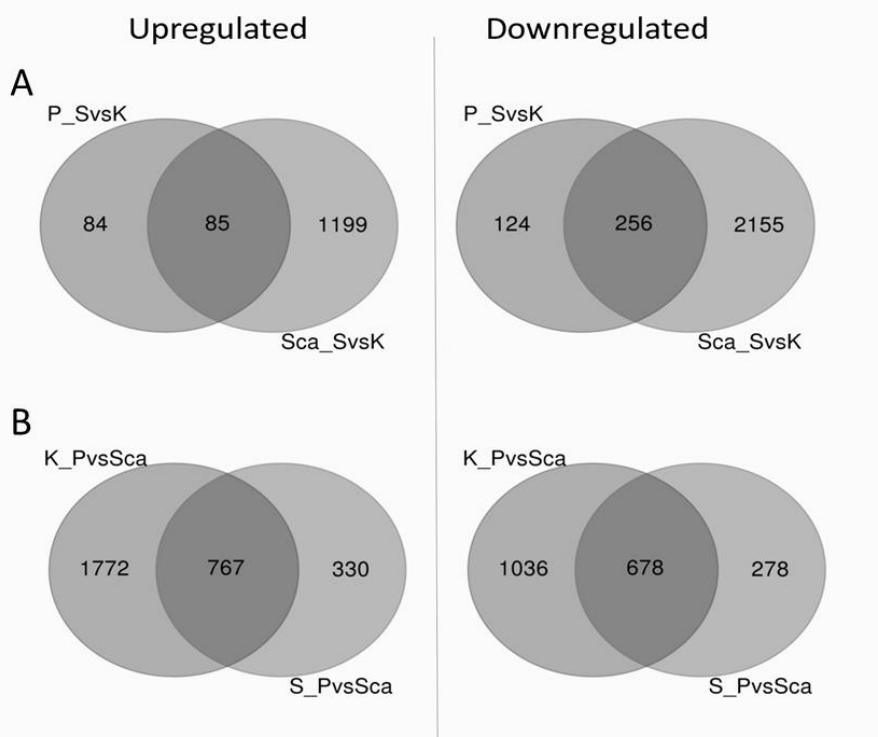

Figure 21 Overview of differentially expressed genes (DEGs) by Venn diagram Venn diagrams depicting the cross-comparison between the number of DEGs (A) in between the control and stress treatment; (B) comparison in between the genotypes. (P – Pakistan; Sca – Scarlett; K – Control; S – Stress).

Significantly enriched GO terms were identified by Singular Enrichment Analysis with AgriGO v.2, the analysis with upregulated DEGs as a response to osmotic stress showed 10 unique GO terms in Scarlett and 15 GO terms in Pakistan. Among them highly enriched GO term was 'carbohydrate metabolic process' (GO 0005975) for Scarlett and 'defense response' (GO 0006952) for Pakistan. Significantly enriched terms shared by both genotypes were hydrolase activity and catalytic activity. Analysis with down-regulated DEGs for Scarlett had 45 GO unique terms with ‘protein phosphorylation’ (GO:0006468) being most significant while no unique GO term was found for Pakistan (**Supplementary Table 1)**. The alcohol forming wax gene (CER 4) was highly significant in both cultivar Scarlett and wild accession Pakistan (**Supplementary Table 2)**.

3.12 Wax and cutin genes expression profile

Pathway for the biosynthesis of cuticles starts in the outer membranes of the plastids of epidermal cells where the $C_{16\text{-}18}$ fatty acids are synthesized. These are exported to ER where the wax and cutin monomers are synthesized. The most common compounds of waxes are primary and secondary alcohols, alkanes, ketones, esters

and aldehydes. While prominent cutin monomers are fatty acids, ω-hydroxy acids (OH) and 9,10 epoxy C_{18} OH. Different kinds of enzymes mediate the process of wax/cutin synthesis step by step.

Table 5 Wax and cutin gene expression profile The expression of important putative wax and cutin genes are tabulated along with their barley ids. The numbers indicate the Log2 Fold Change (Log2 FC) of the corresponding gene expression. (Sca.: Scarlett; Pak.: Pakistan; S: stress; C: control)

Barley Id	Putative Gene	Log_2 FC Sca_S vs. C	Log_2 FC Pak_S vs. C
WAX GENE			
HORVU5Hr1G089230	CER4 (FAR)	4.805399	5.053586
HORVU5Hr1G124820	CER4 (FAR)	8.854075	-
HORVU4Hr1G063420	KCS1	2.044921	-
HORVU1Hr1G016200	CER8, LACS1	2.976834	-
HORVU3Hr1G020800	MAH1	1.981792	-
HORVU3Hr1G074840	WSD1	-0.86327	-
HORVU1Hr1G039820	CER1	6.984711	3.065857
HORVU1Hr1G039830	CER1	3.281033	3.042646
CUTIN GENE			
HORVU1Hr1G075900	DCR	3.79936	-
HORVU3Hr1G056830	GPAT1	3.752673	
HORVU3Hr1G080190	GPAT2	-	1.928283
HORVU1Hr1G016200	LACS1	2.976834	-
HORVU0Hr1G018210	HUB1	-	-
HORVU3Hr1G099950	HUB2	-	-
HORVU3Hr1G085020	CYP86A1	-	-
HORVU2Hr1G072400	CYP77A6	-	-

TRANSPORTORS			
HORVU3Hr1G022800	ABCG32	2.144191	-
HORVU1Hr1G030200	ABCG12	1.96722	
HORVU2Hr1G090960	ABCG11	1.674804	-
HORVU3Hr1G009360	LTP1	-	-
HORVU3Hr1G009490	LTP1	4.565678	-
TRANCRIPTION FACTORS			
HORVU7Hr1G089930	WIN1/SHN1	-	-
HORVU2Hr1G028470	MYB96	-	-

The expression of some of the important genes during the stress along with their barley ids are tabulated (**Table 5**). Wax genes (CER4, CER8, MAH1 and KCS) and cutin genes (DCR and GPAT1) were significantly up-regulated in cultivar Scarlett, while in wild accession Pakistan only CER4 and GPAT2 were up-regulated under osmotic stress. A putative ortholog of WSD 1 (wax ester synthase gene) was most down-regulated in cultivar Scarlett while no effect in wild accession Pakistan. Important cutin gene family Cytochrome P450 under osmotic stress had no effect on gene expression for both individuals. The transcription factors WIN1/SHN1 and MYB96 regulating the cutin/wax biosynthesis showed no effect under osmotic stress. Though most of the genes have no fold change in wild accession Pakistan, the overall expression of wax and cutin genes was higher in Pakistan compared to Scarlett (**Supplementary Table 2**).

Chemical analysis of 4 cm region

Simultaneous to the leaf transcriptomics, the 4 cm region of leaf 2 from POE was analysed for wax and cutin amounts. Cuticular waxes were composed of four main monomer classes: fatty acids, alcohols, aldehydes and esters. A similar deposition trend of wax was observed between the cultivar Scarlett and wild accession Pakistan. A slight increase in the wax amount was deducted under osmotic stress. Wax in cultivar Scarlett increased from 11.75 ± 0.35 $\mu g/cm^2$ to 15.90 ± 2.01 $\mu g/cm^2$ and for

wild accession Pakistan an increase from 11.12 ± 1.07 μg/cm^2 to 17.37 ± 0.54 μg/cm^2 was observed (**Figure 22**A).

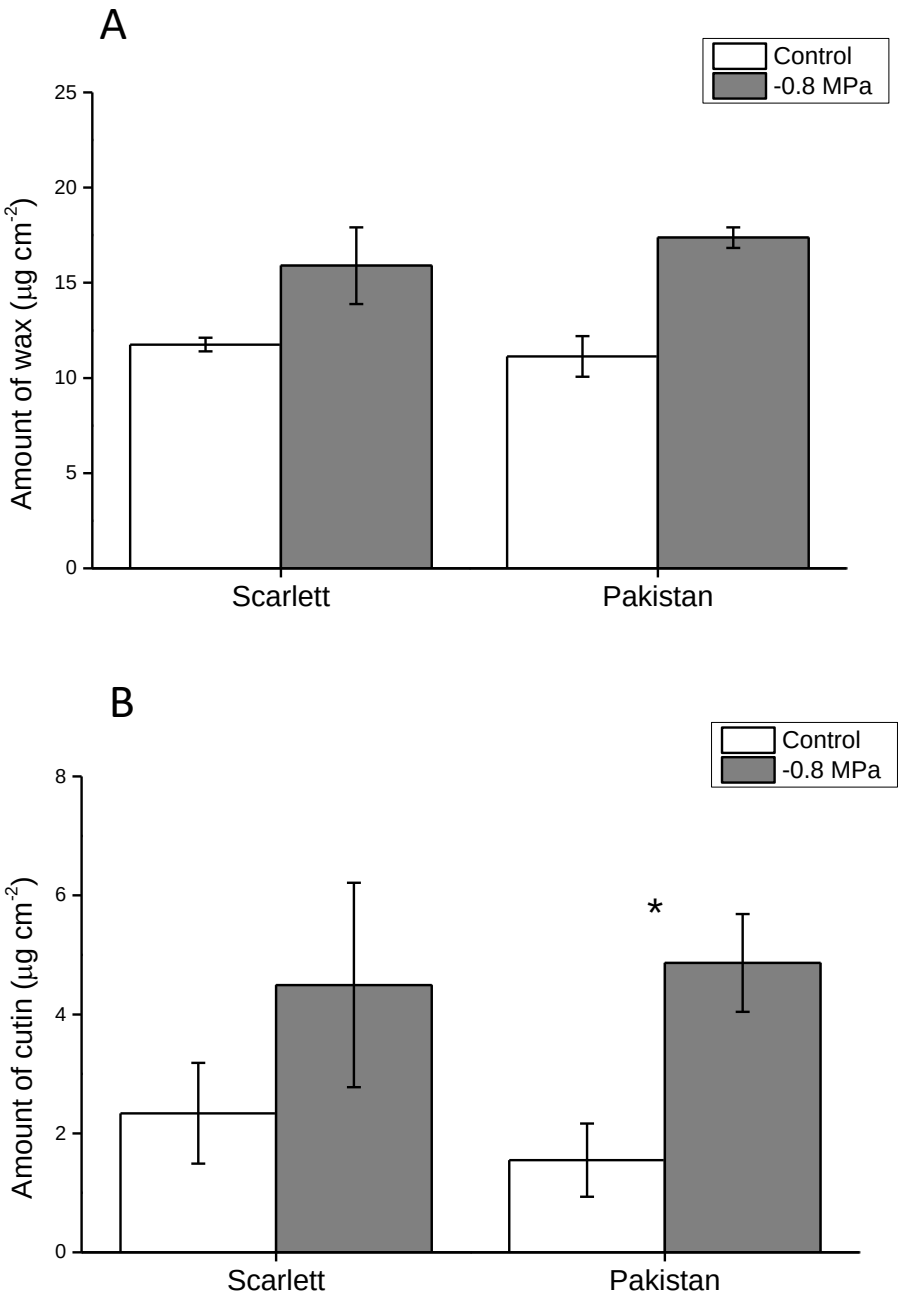

Figure 22 Total amount of wax from 4 cm region (A) Wax and (B) cutin extracted from 4 cm region of leaf 2 of cultivar Scarlett and wild accession Pakistan is represented. Bars indicate means with the corresponding standard deviation. With three replicates, no significant differences were observed between means at a significance level of 0.05 tested in one-way ANOVA (Fisher's LSD test).

The leaves used for wax analysis were subsequently used for cutin extraction with chloroform as described in materials (2.8). The deposition of cutin increased during osmotic stress. For cultivar Scarlett cutin increased from 2.34 ± 0.84 μg/cm^2 to 4.49 ±

1.17 μg/cm^2 and for Pakistan a significant increase from 1.55 ± 0.62 μg/cm^2 to 4.85 ± 0.82 μg/cm^2 was observed (**Figure 22**B).

4 Discussion

The effect of osmotic stress on morphological, physiological and chemical levels was studied on 12-d old barley plants of two different genotypes. Stress was induced by the application of PEG 8000 on day 6 by reducing the water potential to -0.8 MPa. During water stress plants tend to have lesser water content reduction, decreased photosynthetic activity, enhanced stomatal closure, accumulation of compatible solutes and more production of wax/cutin (Sallam et al., 2019). Here the investigation was carried out to check whether the stress sensed by roots increased the wax and cutin amounts and reduced transpiration rates. These characteristics were assessed in barley plants of cultivar Scarlett and compared with wild accession Pakistan.

4.1 Growth response

As a result of negative water potential, the first phenotype observed was the reduced growth of the plants. The effect of root length has been addressed in the previous study which showed a significant reduction by 10% (Kreszies et al., 2019). Here, it was noted that by the day of reducing water potential, the development of leaf 1 is almost complete while leaf 2 continues to develop in the stress environment because of which growth of leaf 2 was significantly affected (**Figure 6** A-C). These phenotypic modifications are regulated by turgor-driven cell wall extension. During limited water availability, the cell expansion is inhibited and is associated with the low turgor pressure resulting in reduced growth (Jaleel et al., 2009; Lockhart, 1965; Neumann et al., 1994; Oliverira et al., 2013). Apart from this, the plastic properties of cell walls and conductivities of cell membranes change due to low water potential, which affects the cell elongation (Nonami & Boyer, 1990). From microscopic observations of barley leaf imprints, it was evident that the cell elongation was reduced as a response to osmotic stress (**Figure 7)**. As a result of reduced cell elongation more cells were formed hence the density of the stomatal cells and epidermal cells were increased especially in leaf 2 by 70% for cultivar Scarlett and 28% for wild accession Pakistan (**Supplementary Figure 3**). Our measurements were consistent with past studies showing an increased cell density by 70% in Sorghum (Jordan et al., 1984) and 23% in barley cv. Quench (Even et al., 2018).

4.2 Stomatal conductance and Photosynthesis

Leaf transpiration drives the uptake of water through roots and transport throughout by xylem vessels. In response to osmotic stress, a 3-fold reduction in stomatal transpiration was observed (**Figure 9 and Supplementary Figure 1**) as a result of partial stomatal closure. Closure of stomata associated with decreased transpiration under stress is perceived in most plant species (Almousa, 2017; Kusvuran, 2014; Miyashita et al., 2005; Turan et al., 2009; Yeo et al., 1985). Stomatal closure is mediated either by loss of turgor (hydropassive) or by ABA-mediated (hydroactive) mechanisms. Osmotic stress enhances suberin deposition in barley seminal roots (Kreszies et al., 2019, 2020) and Baxter hypothesized that increased suberin in roots as a result of water stress, sends ABA-mediated signals to shoots or by hydraulic signals which affect the stomatal transpiration (Baxter et al., 2009). In the current study, for both control and stress plants the abaxial side had 10-fold lesser stomatal conductance than the adaxial side of the leaf (**Supplementary Figure 1**). A similar response has been reported before in sorghum and sunflower (Turner et al., 1978; Turner & Singh, 1984) and studies on broad bean postulated that possibly environmental stimuli could drive the sensitivity of the stomatal movement between the two sides of the leaves (Wang et al., 1998).

Light is vital for photosynthesis but exposing plants to higher light intensities, decreases the quantum yield, Y(II). Because of high intensity, the activity of photosystem II is declined which results in the decline of Y(II) (Murata et al., 2012). During initial light intensity (<200 µmol m^{-2} s^{-1}) there is no decline in the quantum yield while above the light intensity of PAR (>200 µmol m^{-2} s^{-1}) there is a sharp decline in the yield (**Figure 11**A). The decline above this particular PAR (>200 µmol m^{-2} s^{-1}) is mainly because the plants are not exposed above the intensity of about 140 µmol m^{-2} s^{-1} in the growth chamber because of which the photosynthesis is limited and exhibit higher electron transport rates (**Figure 11**B). Subsequent comparison between the treatment, with a slight decrease in the tendency (because of the drop in the stomatal conductance), but no significant difference observed. There is no considerable difference observed between the treatments because all stomata are not fully closed during stress, so the availability of CO_2 for photosynthesis is not limited which potentially did not affect the quantum yield for the stress plants. A similar observation was obtained between both the cultivar Scarlett and wild accession

Pakistan. Likewise, studies on *Psidium guajava* show that the application of nickel stress affects the stomatal conductance significantly while the net photosynthetic rate was not affected (Bazihizina et al., 2015).

4.3 Residual transpiration

One of the principal functions of the cuticle is to form a barrier against uncontrolled water loss when stomata are closed (Richardson et al., 2007; Schreiber, 2010; Zabka, 2007). Since not all stomata might close perfectly, the transpirational loss of the leaf at minimal stomatal aperture is termed as residual transpiration. In the present study, residual transpiration varied significantly between the cultivar Scarlett and wild accession Pakistan. Wild type having considerably initial lower water loss over time could be a quicker response of stomata's to close compared to cultivar Scarlett when detached (Figure 10). The value 7.95 $x10^{-10}$ m s^{-1} obtained for the cultivar Scarlett in the present study correlated with the barley cultivar Quench under control conditions which was determined to be $8x10^{-10}$ m s^{-1} (Even et al., 2018). The effect of the reduced water potential did not affect the residual transpiration in both the barley types here. A study on the response of residual transpiration of different barley cultivars under the water stress showed different tendencies from no difference to a significant decrease or increase in the transpiration rate (Svenningsson, 1988). Genotypes having lesser residual transpiration become an important trait in selection criteria for the breeding process for generating drought stress-tolerant plants.

4.4 Compatible solutes

As an additional approach, proline was measured as plants tend to accumulate compatible solutes as an adaptive mechanism to cope with the stress. Proline content in leaves increased by 2-fold as a response to osmotic stress (Figure 12). Similarly, barley roots accumulated 2-fold proline when they were subjected to osmotic stress (Kreszies et al., 2020). The osmotic potential of the plant cells is balanced by increased proline accumulation during the water stress. Drought stress studies on cultivar Scarlett had a significant increase in proline amount (Muzammil et al., 2018). Similarly, the leaves of wheat plants tend to accumulate more proline than any other osmo-regulators as a response to different stress environments (Nazarli & Faraji, 2011). They regulate the water loss from the cells and also help to provide the energy for the growth of plants (Basudeb et al., 2019). Key enzyme Pyrroline-5-carboxylate synthase 1 (barley id: HORVU1Hr1G072780) is required for

proline production. It converts glutamate to glutamate 5-semialdehyde an intermediate in the biosynthesis of proline (Arentson et al., 2013). This particular gene was significantly upregulated in barley roots, but there was no fold change difference noted in barley leaf.

4.5 Effect of osmotic stress on leaf wax and cutin

The quantitative wax/cutin amounts and individual monomers detected were identical between cultivar Scarlett and wild accession Pakistan and they were consistent with other barley data published (Espelie et al., 1979; Richardson et al., 2005, 2007; Zabka, 2007). In barley, C_{26} alcohol dominates the wax amounts and in the current study, it amounted to 85% for both Scarlett and Pakistan and fits with previous data (Giese, 1976; Larsson & Svenningsson, 1986; Richardson et al., 2005; Zabka, 2007). We adapted different approaches for expressing the amounts to see if there was a real increase in the synthesis of wax/cutin or the increase was contributed by decreased leaf area because, under drought stress, an increase in the wax coverage could positively strengthen the protective barrier.

SEM images clearly showed stress leaves had denser and protruded wax crystals (**Figure 13**) which are explained by a 30% increase in wax amounts relative to per leaf surface (µg cm^{-2}; (**Figure 15**A). Either an increase or decrease in wax load has been reported previously depending on barley cultivars. Drought stress study by Zabka, 2007 observed a 20% increase in wax load (cv.Bonus), Gonzalez & Ayerbe, 2010 noted a 9% increase while Larsson & Svenningsson, 1986 stated no increase in different barley cultivars. Alternatively, presenting the wax amounts as a whole leaf, µg (esp. leaf 2) a significantly lower amount of deposition was observed under stress (**Figure 14**A). This contrary outcome is due to the effect of reduced leaf area (**Figure 6**D). As a response to osmotic stress, leaf 2 area was decreased by almost 50% for both cultivars which resulted in a 50% lesser wax amount in the whole leaf. These results from both approaches imply that there was no increase in the wax amount due to osmotic stress. The increase in wax coverage per leaf area (µg cm^{-2}) is attributed mainly because of the total leaf area reduction but not because of the increased wax biosynthesis. Considering the response of osmotic stress on cutin coverage, a 10% decrease in the whole leaf 1 cutin amount (µg) for both genotypes was observed as the result of 10% decrease in leaf area. Contradictorily leaf 2 cutin amounts averaged the same for control and stress leaves despite the decrease in leaf area which implies

more synthesis of cutin by leaf 2 (**Figure 16**A). Among the cutin monomers, ω hydroxylated compounds comprised a major part. Although $C_{18:1}$ ω hydroxy acid constituted a significant percentage, the majority of cutin was composed of 9,10 epoxy ω-C_{18} hydroxy acid. In similar to the current study, the earlier reports indicated that 9,10 epoxy ω-C_{18} OH accounted for 33.8% (Espelie et al., 1979) and 29% in cv. Golf (Richardson et al., 2007). The overall wax amount was 9.2-fold and 10.5-fold more comparatively to the cutin amount for Scarlett and Pakistan. A possible explanation could be that cutin deposition begins during the early stages of epidermal cell development where they are predominated and when elongation ceases and goes past the POE region the cutin deposition is minimized while wax deposition becomes prevalent (Richardson et al., 2005, 2007).

4.6 Correlation between the wax load and residual leaf transpiration

The barrier properties of cuticles are established by the cuticular waxes, while the cutin membrane gives mechanical stability to the waxes. We observed that the permeance did not decrease with increasing density of wax content per leaf area (**Figure 10**B**; Figure 15**A). In the past, there has been a lot of research focusing on the correlation between wax load and transpiration and published both positive and negative correlation depending on plant species. For example, in sorghum, a negative correlation was observed by (Jordan et al., 1984) whereas studies in tomatoes showed waxes provide a minor contribution to the transpiration barrier (Vogg et al., 2004). Analysis of different plant species by (Schreiber & Riederer, 1996) indicated no correlation between the cuticle thickening and transpiration. It was also proposed that rather than the wax amount, the structure and orientation of wax crystals might play a role in transpiration while the excess amount of wax during stress could have other positive effects (Sanchez et al., 2001; Schreiber and Riederer 1996). Nevertheless, denser wax and cutin coverage per leaf area could benefit the leaves from reduced light absorption and warming up of the leaves.

4.7 Gene expression studies

The analysis of wax deposition pattern on different leaf segments displayed that the wax increases post-emergence, later the deposition rate is constant over the leaf blade (**Figure 18**). Likewise, Richardson and co-workers analyzed the developing stages of barley leaf and affirmed that the deposition of cuticular waxes starts from the portion

that is enclosed within the sheaths of older leaf and the expression of wax genes commences from this region. Following, the wax deposition increases post-emergence, after which the rate is constant over the leaf blade (Richardson et al., 2005). Since the expression of wax genes commences from the POE region, the first 2 cm region was used for RNA-Seq. Genes involved in VLCFAs and wax biosynthesis pathways were obtained for example CER1, CER6/CUT1, KCR, HCD and so on (**Supplementary Table 2**A). Overexpression of these genes increases the wax production and enhances drought tolerance (Islam et al., 2009; M. Wang et al., 2016; Y. Wang et al., 2020). In the current study due to osmotic stress, for Scarlett CER1, CER6/CUT1, KCS1, CER4, GL1 had higher expression and in Pakistan, only CER1 and CER4 were overexpressed (**Table 5**). The subfamily of ATP proteins, ABC half transporters (ABCG11/ABCG12) are involved in the transport of wax from epidermal cells across the plasma membrane (Chen et al., 2011) and they were overexpressed for Scarlett while no expression changes observed for Pakistan. Some of the important cutin genes DCR, LACS1 and GPAT were highly expressed in Scarlett while in Pakistan only GPAT was highly expressed (**Table 5**). These genes were involved in the cutin biosynthesis pathway (Lu et al., 2009; Panikashvili et al., 2009; Yang et al., 2012). Altogether the results of RNA-Seq data indicated most of the putative wax and cutin genes were upregulated in Scarlett but showed weaker response in Pakistan. However the results of chemical analysis indicated the increase of wax and cutin amounts as a response to osmotic stress in both Scarlett and Pakistan (**Figure 22**). This different behaviour between genotypes was previously observed in roots where Scarlett had higher suberin gene expression with enhanced suberization while Pakistan had weaker response and less suberization (Kreszies et al., 2019, 2020). The higher wax and cutin genes observed could be possibly triggered by the stress sensed by the roots.

Apart from wax/cutin genes, changes in the expression levels of aquaporin genes, proteins regulating stomatal closure, proline genes were analyzed. Aquaporins are water channels which regulate the water movement through the cell-cell pathway and here the total transcripts of aquaporin genes during stress were slightly lesser compared to control treatment. Lower expression of aquaporin during abiotic stress was found to preserve the water content by minimizing transpiration through stomatal regulation linked with ABA signals and also they enhance photosynthesis

(Alexandersson et al., 2005; Jang et al., 2004; Kapilan et al., 2018; Moshelion et al., 2015). The overall expression of leaf aquaporin genes in Pakistan was slightly higher compared to Scarlett which was in accordance with root aquaporin expression (**Supplementary Table 2**C and Kreszies et al., 2020). Barley root had 2-fold higher expression of aquaporin compared to leaf and this was in accordance with previous studies (Heinen & Ye, 2009; Lian et al., 2006; Perrone et al., 2012). Further insight into this trait of aquaporin could be potentially used for improving drought-tolerant plants.

During drought stress, the expression of ABA receptor proteins, Ca^{2+} and K^{+} channel proteins will be altered for effective stomatal closure to prevent excessive water loss (Daszkowska-Golec & Szarejko, 2013; Hosy et al., 2003; Ooi et al., 2017). In the present study, the stomatal transpiration was declined by 3-fold as a response to osmotic stress which was associated with higher expression of ABA receptor proteins for both genotypes and down-regulation of proteins involved in Ca^{2+} and K^{+} channels especially for Scarlett (**Supplementary Table 2**D).

Apart from this, the expression of the key proline gene Pyrroline-5-carboxylate synthase 1 (HORVU1Hr1G072780) was similar between control and stress for both genotypes. Proline is an important compatible solute accumulated during stress for an osmotic adjustment (Bates, 1973). Although no expression change of the proline gene, the barley leaf proline concentration was increased significantly similar to barley root proline (Kreszies et al., 2020).

4.8 Conclusion – Response of barley root and shoot to osmotic stress

Assessing the drought stress tolerance at the seedling stage is an important trait as it later affects the growth and grain yield. The leaf and root characteristics are mainly focused during this seedling stage.

Water supplied by roots contributes to the overall water balance of the shoot (Steudle, 2000). In many crops, the root system is the first organ to recognize water stress (Basu et al., 2016). Recent studies on 12-d old barley plants as a response to osmotic stress (ψ: -0.8 MPa), show a significantly reduced root length and enhanced suberization sealing the root apoplastic water uptake thus avoiding water loss. Corresponding transcriptomics studies specified significantly upregulated suberin genes as a response to water deficit conditions (Kreszies et al., 2019, 2020). And the study was

extended in both modern cultivars and wild barley varieties and was indicated that the wild barley was well adapted to osmotic stress compared to modern cultivar as they responded differently. Here, the study was extended to aerial parts focusing on the leaf adjustment to osmotic stress for cultivated barley (Hordeum vulgare spp. vulgare) and compared with wild barley (Hordeum vulgare spp. Spontaneum).

Plant cuticles cover the aerial parts of plants and act as the main barrier against the water loss from leaves. Here, the investigation was carried whether barley cutin and waxes play a role in drought adaptation to cope with the stress. Given the present findings, it is concluded that the osmotic stress attained by PEG8000 decreases the overall plant growth. Similar to root length, epidermal leaf cell elongation is affected significantly, especially for growing leaf 2 of both Scarlett and Pakistan. Decreased leaf length resulted in accumulation of denser wax crystals over the leaf which correlated with an increase in wax and cutin amounts. However, increased wax/cutin amounts did not alter the cuticular transpiration. Possibly, enhanced coverage could benefit the leaves from excess light absorption and reduce the warming up of leaves. The residual transpiration was slightly lower in wild type which may indicate the better tolerance of wild barley compared to cultivated barley. This trait could potentially benefit for breeding programs in developing drought tolerant plants. Scarlett had a higher expression of wax and cutin genes while Pakistan had a weaker expression which was in accordance with root suberin gene expression and leaf aquaporin expression was 2 fold lesser compared to root aquaporin (Kreszies et al., 2020). Studying the different segments of the leaf, it was noted that the deposition of wax increases linearly post-emergence and later the deposition rate stayed constant over the leaf blade.

5 Summary

Abiotic stress, especially climate change, is the main limiting factor in modern agriculture. Global climatic changes result in rising temperatures, greater evapotranspiration and increased prevalence of drought. Barley, one of the earliest domesticated crops makes a perfect model organism for various genetic and physiological studies due to its adaptations to various habitats especially to abiotic stress environments of cold, drought, alkalinity and salinity as it is highly resistant. Assessing the drought stress tolerance at the seedling stage is an important trait as it later affects the growth and grain yield. The leaf and root characteristics are mainly focused during this seedling stage. Previous studies showed that 12-d old barley seminal roots had significantly reduced root length and enhanced suberization sealing the root apoplastic water uptake thus avoiding water loss. Here, the investigation was carried on to aerial parts focusing on the leaf adjustment to osmotic stress induced by PEG8000.

Plant cuticles such as cutin and waxes cover aerial parts of plants thereby acting as a main barrier against water loss from leaves. Different experimental approaches (analytical, physiological and transcriptomics study) were carried out to investigate whether barley cutin and waxes play a role in drought adaptation to cope with the stress. Given the present findings, it is concluded that the osmotic stress attained by PEG8000 decreases the overall plant growth. Similar to root length, epidermal leaf cell elongation is affected significantly, especially for growing leaf 2 of both barley varieties. Decreased leaf length resulted in the accumulation of denser wax crystals over the leaf which correlated with an increase in wax and cutin amounts. This concurs with the increased wax and cutin genes. Stomatal conductance decreased significantly, whereas increased wax/cutin amounts did not alter the residual transpiration. Possibly, enhanced coverage could benefit the leaves from excess light absorption and reduce the warming up of leaves. Contradictory to the popular conclusions, from the present finding the increased wax/cutin amounts need not to be associated with decreased cuticular transpiration. Here, the residual transpiration was slightly lower in wild barley which may indicate the better tolerance of those plants in drought prone regions. This trait could potentially benefit for breeding programs in developing a more drought-tolerant crop for agriculture.

6 Supplementary

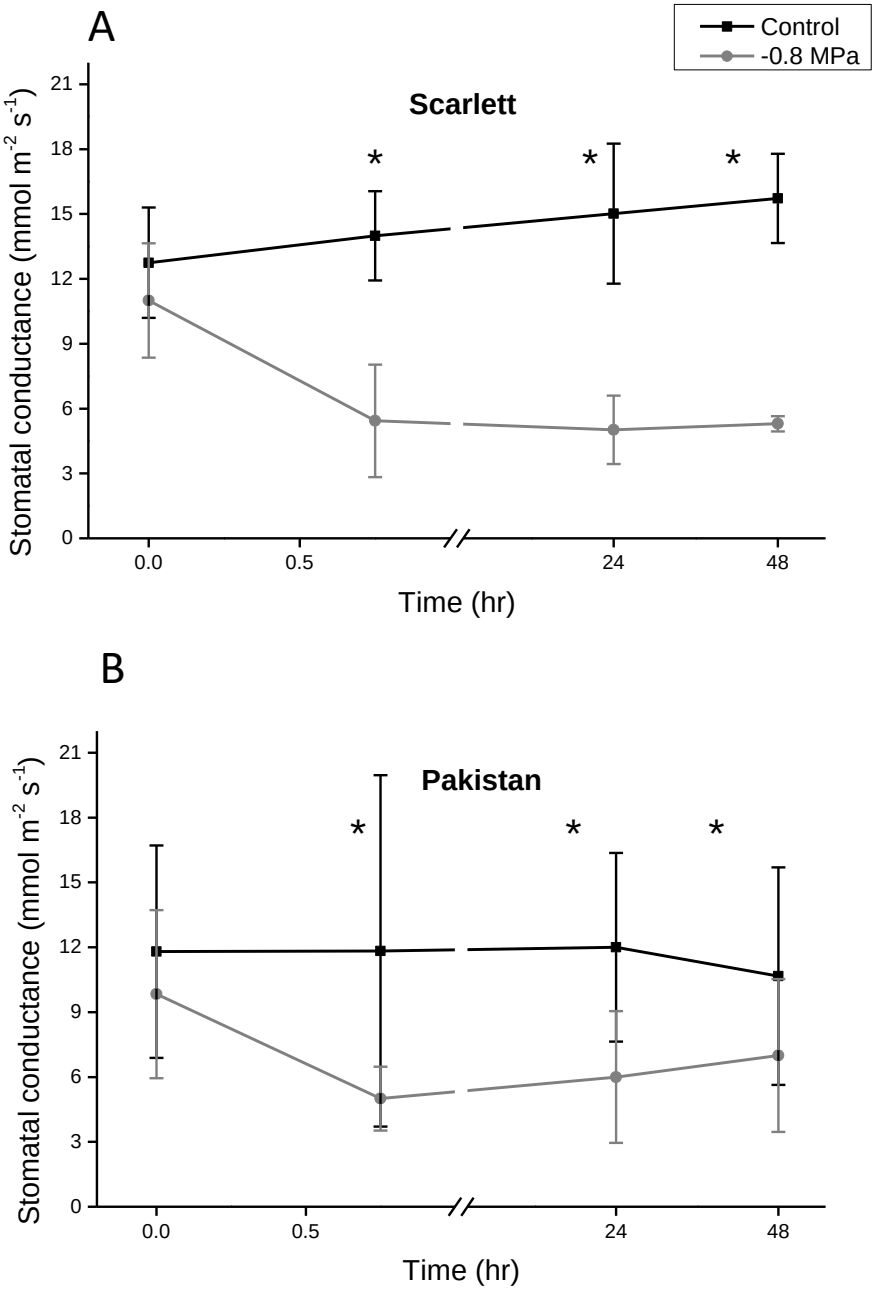

Figure S1 Effect of osmotic stress on stomatal transpiration on the abaxial side of the leaf Abaxial leaf transpiration for (A) cultivar Scarlett and (B) wild accession Pakistan. Black symbols indicates the transpiration of control plants and grey symbols indicate the transpiration of the osmotically stressed plants. The asterisk represents a significant difference between the control and stress leaf. With a minimum of three replicates, the significant differences between means are at a significance level of 0.05 tested in one-way ANOVA (Fisher's LSD test).

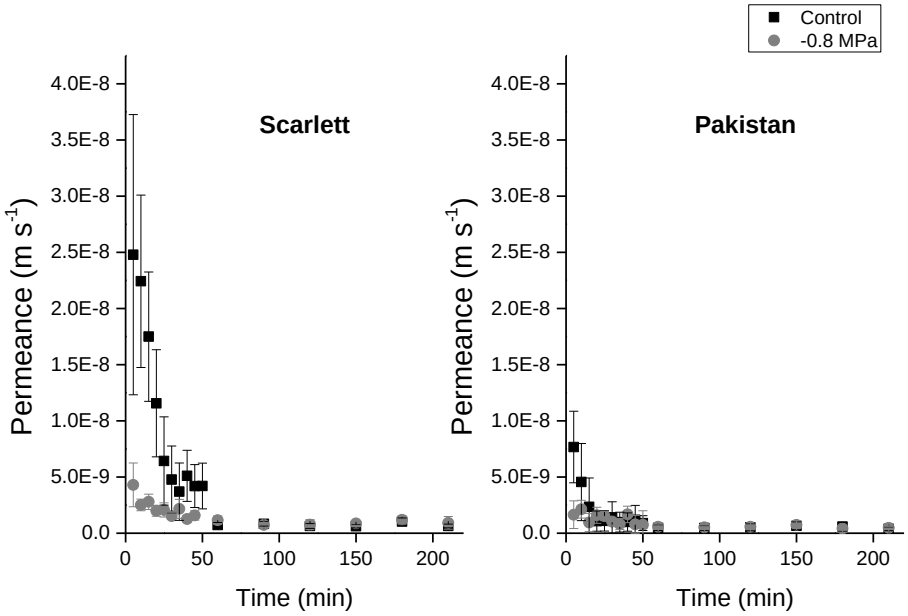

Figure S2 Residual transpiration of detached leaves The graph shows the minimum leaf conductance for both cultivars. The initial higher permeance is due to the water loss through the open stomata. After 1hr transpiration is controlled by cuticles and a few unclosed stomata's Black square symbol indicates the effect of control plants and the grey circle symbol indicates the effect of stressed plants.

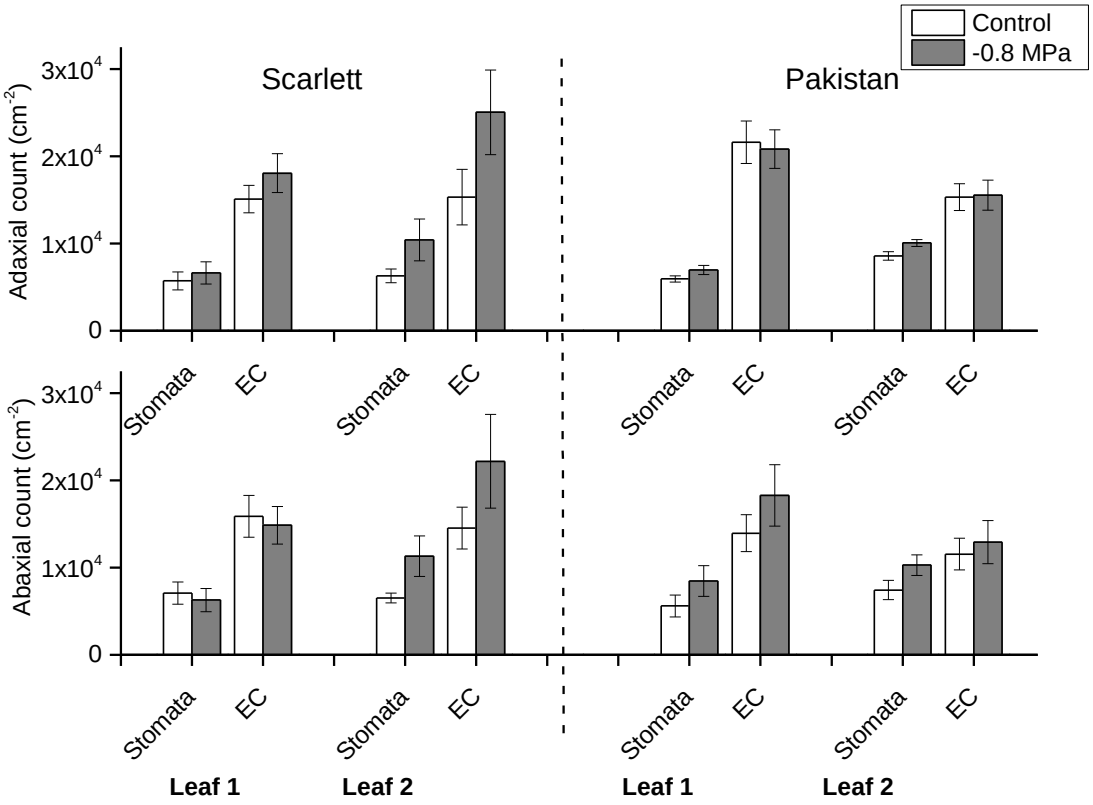

Figure S3 Stomatal cells and epidermal cell counts over adaxial and abaxial sides of barley leaves The distribution of stomatal cells and epidermal cells were counted on the abaxial and adaxial side of the leaf by collodium imprints. Bars indicate means of minimum four replicates with the corresponding standard deviation there was no significant differences between means are at significance level of 0.05 tested in one-way ANOVA (Fisher's LSD test).

Table S1 Cross comparison of enriched GO terms from DEGs of barley leaves of cultivar Scarlett and wild accession Pakistan.

GO terms obtained by Gene ontology enrichment analysis and cross compared between the genotypes at FDR<0.05.

Onto: Ontology; P: Biological process; F: molecular function; C: cellular component; Sca.: Scarlett; Pak.: Pakistan; FDR: false discovery rate

(A) Cross comparison of enriched GO terms from upregulated DEGs

No	GO Term	Onto	Description	Sca.	Pak.	FDR	Num	FDR	Num
1	GO:0005975	P	carbohydrate metabolic process			1.40E-05	109	---	---
2	GO:0044264	P	cellular polysaccharide metabolic process			0.038	22	---	---
3	GO:0016798	F	hydrolase activity, acting on glycosyl bonds			5.80E-07	81	0.015	16
4	GO:0004553	F	hydrolase activity, hydrolyzing O-glycosyl compounds			7.30E-06	72	0.015	15
5	GO:0003824	F	catalytic activity			3.20E-05	755	0.047	127
6	GO:0016787	F	hydrolase activity			0.00061	254	---	---
7	GO:0016757	F	transferase activity, transferring glycosyl groups			0.00061	75	---	---
8	GO:0048046	C	apoplast			0.018	15	---	---
9	GO:0030312	C	external encapsulating structure			0.028	16	---	---
10	GO:0005618	C	cell wall			0.028	16	---	---
11	GO:0006952	P	defense response			---	---	0.0036	10
12	GO:0050896	P	response to stimulus			---	---	0.037	28
13	GO:0030145	F	manganese ion binding			---	---	4.30E-05	9
14	GO:0045735	F	nutrient reservoir activity			---	---	0.0006	9
15	GO:0016702	F	oxidoreductase activity, acting on single donors with incorporation of molecular oxygen, incorporation of two atoms of oxygen			---	---	0.0033	5
16	GO:0051213	F	dioxygenase activity			---	---	0.0033	5

17	GO:0016701	F	oxidoreductase activity, acting on single donors with incorporation of molecular oxygen			---	---	0.0065	5
18	GO:0030414	F	peptidase inhibitor activity			---	---	0.015	6
19	GO:0004866	F	endopeptidase inhibitor activity			---	---	0.015	6
20	GO:0061135	F	endopeptidase regulator activity			---	---	0.015	6
21	GO:0061134	F	peptidase regulator activity			---	---	0.015	6
22	GO:0016491	F	oxidoreductase activity			---	---	0.033	39

(B) Cross comparison of enriched GO terms from down regulated DEGs

No	GO Term	Onto	Description	Sca.	Pak.	FDR	Num	FDR	Num
1	GO:0006468	P	protein phosphorylation			4.90E-09	123	---	---
2	GO:0016310	P	phosphorylation			6.40E-09	129	---	---
3	GO:0036211	P	protein modification process			1.10E-08	139	---	---
4	GO:0006464	P	cellular protein modification process			1.10E-08	139	---	---
5	GO:0043412	P	macromolecule modification			9.00E-08	139	---	---
6	GO:0006793	P	phosphorus metabolic process			9.00E-08	141	---	---
7	GO:0006796	P	phosphate-containing compound metabolic process			2.10E-07	139	---	---
8	GO:0044706	P	multi-multicellular organism process			0.0018	17	---	---
9	GO:0009875	P	pollen-pistil interaction			0.0018	17	---	---
10	GO:0008037	P	cell recognition			0.0018	17	---	---
11	GO:0048544	P	recognition of pollen			0.0018	17	---	---
12	GO:0009856	P	pollination			0.0018	17	---	---
13	GO:0044702	P	single organism reproductive process			0.0019	17	---	---
14	GO:0044282	P	small molecule catabolic process			0.0094	8	---	---
15	GO:1901565	P	organonitrogen compound catabolic process			0.014	10	---	---
16	GO:0016054	P	organic acid catabolic process			0.018	7	---	---

17	GO:0044703	P	multi-organism reproductive process			0.022	17	---	---
18	GO:0000003	P	reproduction			0.023	17	---	---
19	GO:0022414	P	reproductive process			0.023	17	---	---
20	GO:0032501	P	multicellular organismal process			0.025	18	---	---
21	GO:0004672	F	protein kinase activity			3.90E-09	123	---	---
22	GO:0016301	F	kinase activity			3.90E-09	131	---	---
23	GO:0016773	F	phosphotransferase activity, alcohol group as acceptor			5.30E-09	129	---	---
24	GO:0016772	F	transferase activity, transferring phosphorus-containing groups			2.80E-07	136	---	---
25	GO:0030554	F	adenyl nucleotide binding			2.90E-05	174	---	---
26	GO:0032559	F	adenyl ribonucleotide binding			2.90E-05	174	---	---
27	GO:0016740	F	transferase activity			6.80E-05	199	---	---
28	GO:0097367	F	carbohydrate derivative binding			0.00013	184	---	---
29	GO:0032549	F	ribonucleoside binding			0.00016	179	---	---
30	GO:0017076	F	purine nucleotide binding			0.00016	180	---	---
31	GO:0032555	F	purine ribonucleotide binding			0.00016	179	---	---
32	GO:0032553	F	ribonucleotide binding			0.00016	182	---	---
33	GO:0032550	F	purine ribonucleoside binding			0.00016	179	---	---
34	GO:0001883	F	purine nucleoside binding			0.00016	179	---	---
35	GO:0001882	F	nucleoside binding			0.00016	179	---	---
36	GO:0005524	F	ATP binding			0.00047	146	---	---
37	GO:0000166	F	nucleotide binding			0.00072	205	---	---
38	GO:1901265	F	nucleoside phosphate binding			0.00072	205	---	---
39	GO:0036094	F	small molecule binding			0.0011	205	---	---
40	GO:0003824	F	catalytic activity			0.0037	436	---	---
41	GO:0035639	F	purine ribonucleoside triphosphate binding			0.0038	151	---	---
42	GO:0005215	F	transporter activity			0.0067	64	---	---
43	GO:0030246	F	carbohydrate binding			0.01	25	---	---

44	GO:0004674	F	protein serine/threonine kinase activity			0.014	15	---	---
45	GO:0004197	F	cysteine-type endopeptidase activity			0.028	5	---	---

Table S2 Complete list of (A) wax; (B) cutin; (C) aquaporin; (D) stomatal gene DEGs with their Transcripts per million (TPM)

Data indicate means of minimum 4 replicates with the corresponding standard deviation. Significant difference is given by log2foldchange (Log_2FC), where, DEG: Differentially expressed genes; TPM: transcripts per million; P_S vs K : Pakistan Stress vs Control ; Sc_S vs K : Scarlett Stress vs Control; P-K: Pakistan control; P-S: Pakistan stress; Sc-K: Scarlett control; Sc-S: Scarlett stress; SD: Standard Deviation

(A) DEGs of corresponding wax genes with their Transcripts per million (TPM)

				DEG		TPM							
				Log_2FC									
AGI	**barley id**	**gene specific. abb**	**Pathway**	**P_S vsK**	**Sc_S vsK**	P-K	SD	P-S	SD	Sc-K	SD	Sc-S	SD
Os10g0363300	HORVU3Hr1G105880	ACC1	Acetyl CoA carboxylase FATB	--	1.13	154.93	44.83	154.21	10.03	58.14	30.24	112.51	2.77
AT1G08510	HORVU7Hr1G084830	FATB	acyl acyl carrier protein thioesterase	--	1.62	67.41	22.92	149.73	44.81	33.63	13.72	95.74	11.66
At1g68530	HORVU4Hr1G067340	KCS6, CER6, CUT1		0.00	2.68	158.88	77.95	315.59	94.53	30.24	21.84	153.09	21.95
At1g02205	HORVU1Hr1G039820	CER1	aldehydes to alkane	3.07	6.98	40.60	23.53	310.55	135.71	1.44	1.10	172.95	48.37
	HORVU1Hr1G039830			3.04	3.28	0.18	0.23	1.92	1.70	0.00	0.00	0.76	0.10
At3g544540	HORVU5Hr1G089230	CER4 (FAR)	alcohol forming FAR	--	4.81	770.14	271.57	1187.43	395.07	87.33	97.78	705.73	79.87
	HORVU5Hr1G124820			5.05	8.85	3.88	4.12	78.57	21.87	0.05	0.10	68.93	24.36
	HORVU3Hr1G002040			--	--	13.03	5.82	23.65	13.36	8.19	4.24	20.30	2.96
At1g01120	HORVU4Hr1G063420	KCS1	VLCFA synthesis is regulated by KCS	--	2.04	251.50	72.19	273.43	65.82	71.57	64.45	186.85	35.26
At2g47240	HORVU1Hr1G016200	CER8, LACS1	long-chain fatty acid metabolism	0.00	2.98	90.83	27.91	139.09	26.10	12.87	6.51	96.14	22.20

	HORVU1Hr1G089710	KCS 9		--	--	17.47	1.61	17.25	0.76	32.22	14.40	15.49	1.64
Zm00001d020557	HORVU5Hr1G063820	GL1	alkane and aldehyde biosynthetic process	--	1.38	74.61	22.50	112.82	24.89	30.12	14.32	70.65	5.86
At3g55360	HORVU3Hr1G013790	CER10 (ECR)		--	--	188.25	80.73	281.34	122.00	193.71	43.57	254.52	22.64
At1g57750	HORVU3Hr1G020800	MAH1	2 alco and ketones	--	1.98	0.95	0.71	2.39	1.13	0.36	0.19	1.66	0.62
Os01g0770100	HORVU3Hr1G074840	WSD1	wax ester synthase	--	-0.86	9.68	2.52	14.60	2.89	13.73	2.31	7.52	2.62
	HORVU3Hr1G074910			--	--	28.66	5.86	45.22	13.63	41.71	4.04	25.93	2.43
Os04g0483500	HORVU2Hr1G083740	KCR1	b-ketoacyl-CoA reductase,wax biosynthesis,FA elongatio	--	--	0.00	0.00	0.00	0.00	0.00	0.00	0.00	0.00
Os11g0115400	HORVU3Hr1G009360	LTP1	Lipid transfer protein	--	--	7.56	4.52	17.60	11.96	2.45	1.35	12.16	3.72
	HORVU3Hr1G009490			--	4.57	67.75	38.48	165.14	105.49	10.12	10.39	115.58	31.40
	HORVU3Hr1G009370			--		0.07	0.08	0.14	0.19	0.00	0.00	0.07	0.08
At1g17840	HORVU2Hr1G090960	ABCG11	Wax export from PM	--	1.67	47.69	18.61	77.11	33.90	20.44	11.83	56.43	4.06
At1g51500	HORVU1Hr1G030200	ABCG12		--	1.97	76.21	52.56	230.79	133.79	32.33	15.53	115.30	16.65
At1g15360	HORVU7Hr1G089930	WIN1/SHN1		--	--	0.55	0.21	0.41	0.10	0.67	0.39	0.33	0.29
At5g25390	HORVU6Hr1G038120	SHN2/SHN3	transcriptional regulator of KCS1,CER1,CER2	--	--	0.76	0.16	0.92	0.20	0.82	0.24	0.83	0.52
At5g62470	HORVU2Hr1G028470	MYB96		--	--	6.78	4.52	1.84	0.84	4.68	3.08	3.26	1.62
At2g26250	HORVU4Hr1G076940	FDH/KCS10	3-KETOACYL-COA SYNTHASE 10	--	--	361.34	108.60	382.66	28.41	265.69	223.56	513.24	66.33

(B) DEGs of corresponding cutin genes with their Transcripts per million (TPM)

				DEG		**TPM**							
				Log_2FC									
AGI	**barley id**	**gene specific. abb**	**Pathway**	**P_SvsK**	**Sc_SvsK**	P-K	SD	P-S	SD	Sc-K	SD	Sc-S	SD
At2g44950	HORVU0Hr1G018210	HUB1/RDO4											
At2g47240	HORVU1Hr1G016200	LACS1	long-chain fatty acid metabolic process,	--	2.98	90.83	27.91	139.09	26.10	12.87	6.51	96.14	22.20

			wax and cutin biosyntheitc process										
At1g51460	HORVU1Hr1G030200	WBC13 / ABCG13		--	1.97	76.21	52.56	230.79	133.79	32.33	15.53	115.30	16.65
At5g23940	HORVU1Hr1G075900	PEL3/DCR	cutin biosynthetic process	--	3.80	6.54	1.74	20.15	9.95	0.45	0.38	6.81	3.63
At5g04630	HORVU2Hr1G072400	CYP77A6, CYP77A4		--		0.03	0.07	0.08	0.09	0.05	0.10	0.08	0.10
At1g17840	HORVU2Hr1G090960	WBC11 / ABCG11 / DSO/COF1	cutin transport, response to abscisic acid	--	1.67	47.69	18.61	77.11	33.90	20.44	11.83	56.43	4.06
At2g26910	HORVU3Hr1G022800	ABCG32/PEC1	cuticle development	--	2.14	0.78	0.19	2.86	1.69	0.61	0.35	2.46	0.49
At1g72970	HORVU3Hr1G035730	HTD	oxidation-reduction process	--	3.39	17.52	7.61	20.98	12.73	2.58	2.79	12.12	1.27
At1g06520	HORVU3Hr1G056830	sn-2-GPAT1			3.75	37.73	24.81	50.96	13.21	9.62	10.23	61.16	14.35
At1g02390	HORVU3Hr1G080190	GPAT2		1.93	--	1.02	0.10	4.05	1.00	2.04	1.02	2.79	0.66
At1g55250	HORVU3Hr1G099950	HUB2		--	--	8.23	0.79	8.68	2.33	13.05	6.31	9.86	1.33
At4g34100	HORVU7Hr1G116420	SUD1, CER9		--	--	45.22	1.43	43.58	5.38	71.86	30.25	56.40	7.16
At3g01140	HORVU4Hr1G049630	MYB106/NOK		--	--	0.00	0.00	0.00	0.00	0.11	0.21	0.23	0.46
	HORVU4Hr1G089610			--	--	0.00	0.00	0.00	0.00	0.00	0.00	0.00	0.00
	HORVU5Hr1G057590			--	3.23	1.87	0.67	4.28	2.34	0.34	0.39	2.43	0.56
At1g49430	HORVU5Hr1G099350	LACS2		--	--	0.66	0.40	0.72	0.56	2.03	0.66	0.83	0.47
	HORVU6Hr1G001310			--	--	0.00	0.00	0.00	0.00	0.00	0.00	0.00	0.00
At4g00400	HORVU6Hr1G006810	sn-2-GPAT8		--	--	54.93	7.06	62.86	7.58	46.21	4.39	39.25	4.88
At5g25390	HORVU6Hr1G038120	SHN3		--	--	0.76	0.16	0.92	0.20	0.82	0.24	0.83	0.52
At2g45970	HORVU6Hr1G064170	CYP86A8/LCR		--	--	0.02	0.04	0.86	0.70	0.11	0.14	0.77	0.65
At4g00360	HORVU6Hr1G064170	CYP86A2		--	--	0.55	0.21	0.41	0.10	0.67	0.39	0.33	0.29
At1g15360	HORVU7Hr1G089930	WIN1/SHN1		--	--	1.67	0.50	2.02	0.56	1.96	0.59	1.58	0.24
	HORVU7Hr1G089930			--	--								
				--	--								
	HORVU7Hr1G016870	ABCG31		--	--								

AT5G58860	HORVU3Hr1G085020	CYP86A1	fatty acid ω-hydroxylase encoding gene CYP86A7-2	--	--	0.07	0.14	0.07	0.08	0.00	0.00	0.00	0.00
At4g00400	HORVU6Hr1G006810			--	--	54.93	7.06	62.86	7.58	46.21	4.39	39.25	4.88

(C) DEGs of corresponding aquaporin genes with their Transcripts per million (TPM)

				DEG		**TPM**							
				Log_2FC									
AGI	**barley id**	**gene specific. abb**	**Pathway**	**P_Sv sK**	**Sc_S vsK**	P-K	SD	P-S	SD	Sc-K	SD	Sc-S	SD
At3g61430	no	PIP1;1	PIP1A, PIP1a										
At2g45960	no	PIP1;2	PIP1B, PIP1b										
At1g01620	no	PIP1;3	PIP1C, PIP1c										
At4g00430	no	PIP1;4	PIP1E, PIP1e										
At4g23400	no	PIP1;5	PIP1D, PIP1d										
At3g53420	HORVU0Hr1G011280	PIP2;1	PIP2A, PIP2a			0.00	0.00	0.00	0.00	0.00	0.00	0.00	0.00
	HORVU2Hr1G038740					345.05	58.94	267.09	40.89	359.34	160.89	205.18	37.36
	HORVU2Hr1G089820					0.05	0.10	0.07	0.13	0.37	0.44	0.17	0.21
	HORVU2Hr1G089940					609.60	133.06	381.30	94.66	606.38	167.33	368.16	35.86
	HORVU2Hr1G089970					427.00	130.13	297.92	70.81	277.36	37.12	170.20	35.40
	HORVU5Hr1G027240					0.00	0.00	0.00	0.00	0.00	0.00	0.00	0.00
	HORVU5Hr1G029550					0.00	0.00	0.00	0.00	0.00	0.00	0.00	0.00
	HORVU6Hr1G058930					259.28	64.09	135.57	60.64	252.01	101.38	106.01	19.02
At2g37170	wie 2-1	PIP2;2	PIP2B, PIP2b										
At2g37180	wie2-1	PIP2;3	PIP2C, PIP2c, RD28										
At5g60660	wie2-1	PIP2;4											
At3g54820	no	PIP2;5	PIP2D,PIP2d										

At2g39010	wie 2-1`???	PIP2;6	PIP2E, PIP2e										
At4g35100	HORVU2Hr1G010990	PIP2;7	PIP3			475.98	74.93	257.30	29.58	274.42	96.79	338.82	62.25
At2g16850	wie 2-7	PIP2;8	PIP3B	--	--								
At2g36830	HORVU3Hr1G116790	TIP1;1	γTIP	--	--	2362.37	533.10	1459.12	815.29	1376.74	105.10	856.13	163.37
	HORVU4Hr1G079230			--	--	1299.73	209.60	636.76	177.24	964.15	469.43	897.35	80.24
At3g26520	wie 1:1	TIP1;2	γTIP2, TIP2, SITIP	--	--								
At4g01470	wie 1:1	TIP1;3	γTIP3	--	--								
At3g16240	HORVU0Hr1G032130	TIP2;1	δTIP, δTIP1, AQP1	--	--	0.00	0.00	0.00	0.00	0.00	0.00	0.00	0.00
	HORVU6Hr1G062980			--	--	0.00	0.00	0.00	0.00	0.00	0.00	0.00	0.00
	HORVU7Hr1G081770			--	1.62	674.08	261.45	546.82	146.79	112.92	67.96	306.97	36.93
At4g17340	wie 2	TIP2;2	δTIP2	--	--								
At5g47450	wie 2	TIP2;3	δTIP3	--	--								
At1g73190	HORVU1Hr1G043890	TIP3;1	αTIP	--	--	0.17	0.33	0.00	0.00	0.00	0.00	0.00	0.00
At1g17810	wie 3-1	TIP3;2	βTIP	--	--								
At2g25810	HORVU3Hr1G031620	TIP4;1	-	--	--	0.00	0.00	0.00	0.00	0.00	0.00	0.09	0.18
	HORVU3Hr1G031680			--	2.31	1.68	1.19	3.37	0.97	0.37	0.30	1.80	0.11
	HORVU4Hr1G085250			--	--	58.61	42.29	42.80	7.37	144.07	119.06	38.82	16.31
At3g47440	HORVU2Hr1G097780	TIP5;1	-	--	--	0.05	0.06	0.09	0.11	0.00	0.00	0.00	0.00
At4g19030	HORVU5Hr1G085710	NIP1;1	NLM1	--	--	9.31	3.70	7.74	4.52	29.41	21.79	12.43	2.78
	HORVU7Hr1G043590			--	--	0.00	0.00	0.00	0.00	0.00	0.00	0.00	0.00
	HORVU7Hr1G043600			--	--	0.00	0.00	0.00	0.00	0.00	0.00	0.00	0.00
	HORVU7Hr1G088900			--	--	0.00	0.00	0.00	0.00	0.00	0.00	0.00	0.00
	HORVU7Hr1G121250			--	-2.87	0.09	0.11	0.00	0.00	6.84	4.93	0.51	0.46
At4g18910	wie 1-1	NIP1;2	NLM2	--	--								
At2g34390	no	NIP2;1	NLM4	--	--								
At2g29870	no	NIP2;2	-	--	--								
At1g31885	no	NIP3;1	-	--	--								

At5g37810	no	NIP4;1	NLM4	--	--								
At4g10380	HORVU1Hr1G047100	NIP5;1	NLM6, NLM8	--	3.10	137.84	40.69	106.98	30.07	5.84	5.92	25.74	5.60
	HORVU3Hr1G014440			--	--	0.00	0.00	0.00	0.00	0.00	0.00	0.00	0.00
At1g80760	no	NIP6;1	NIP6, NLM7	--	--								
At3g06100	HORVU3Hr1G001320	NIP7;1	NLM6, NLM8	--	--	0.00	0.00	0.00	0.00	0.00	0.00	0.08	0.17
	HORVU3Hr1G001420			--	--	0.00	0.00	0.00	0.00	0.00	0.00	0.00	0.00
At3g04090	no	SIP1;1	SIP1A	--	--								
At5g18290	no	SIP1;2	-	--	--								
At3g56950	no	SIP2;1	-	--	--								
			Additional homologues, pseudogenes in Col-0	--	--								
At1g52180	HORVU2Hr1G013110			--	--	0.00	0.00	0.00	0.00	0.00	0.00	0.00	0.00
	HORVU3Hr1G038940			--	--	0.00	0.00	0.00	0.00	0.00	0.00	0.00	0.00
	HORVU3Hr1G094900			--	--	4.70	4.17	5.12	2.00	2.90	2.99	1.23	0.31

(D) DEGs of corresponding stomatal genes with their Transcripts per million (TPM)

				DEG		**TPM**							
				Log$_2$FC									
AGI	**barley id**	**gene specific. abb**	**Pathway**	**P_SvsK**	**Sc_SvsK**	P-K	SD	P-S	SD	Sc-K	SD	Sc-S	SD
K+ channels				--	--								
				--	--								
AT5G46240	HORVU3Hr1G028670	KAT 1	voltage-gated potassium channel activity, K channel activity	--	--	2.64	0.35	4.52	0.55	2.56	1.21	2.34	0.49
AT4G18290	refer AT5G46240	KAT2		--	--								
				--	--								

Zm00001d010210	HORVU1Hr1G065250	ZMK2	response to abscisic acid, (")	--	--	101.47	16.89	101.43	18.05	62.21	11.23	61.99	8.65
AT2G25600	HORVU3Hr1G058300	AKT1	voltage-gated potassium channel activity, K channel activity	--	--	0.58	0.14	0.52	0.14	0.25	0.28	0.31	0.26
	HORVU2Hr1G083820			--	--	0.00	0.00	0.00	0.00	0.00	0.00	0.00	0.00
AT5G37500	HORVU7Hr1G040970	GORK	K ion transport (outward channels)	--	-2.50	1.62	0.26	1.09	0.41	2.92	2.06	0.47	0.31
	HORVU7Hr1G040880			--		0.04	0.04	0.00	0.00	0.00	0.00	0.09	0.12
	HORVU7Hr1G040990			--	-1.75	1.87	0.37	2.05	1.06	14.79	5.80	4.41	2.76
AT3G02850	refer AT5G37500	SKOR		--	--								
				--	--								
Ca+ channels					--	--							
				--	--								
AT4G03560		TPC1		--	--								
	HORVU5Hr1G063530			--	--								
	HORVU5Hr1G063510			--	-5.21	0.10	0.11	0.00	0.00	5.70	6.36	0.00	0.00
	HORVU5Hr1G063480			--	-4.26	9.60	4.20	3.29	1.47	49.39	48.84	1.69	1.62
	HORVU5Hr1G063500			--	--								
	HORVU6Hr1G083680			--	-3.53								
				--	--								
				--	--								
ABA regulators					--								
				--									
AT4G33950	HORVU4Hr1G013540	SRK2E, OST1	abscisic acid-activated signaling pathway, stomatal movement	0.70	1.53	15.16	3.30	23.90	1.90	5.92	0.73	16.99	1.78
AT3G14440	HORVU5Hr1G044510	NCED		--	--								
	HORVU5Hr1G092850			--	--								
	HORVU5Hr1G054970			--	--								

	HORVU5Hr1G008050			--	--								
AT1G78390	refer AT3G14440			--	--								
AT4G19230	HORVU0Hr1G016780	CYP707A1	ABA catabolism	--	--								
	HORVU6Hr1G068690			--	--								
AT5G45340	refer AT4G19230	CYP707A3		--	--								
AT4G26080	HORVU1Hr1G080290	ABI1		--	--								
	HORVU3Hr1G050340			--	--	31.78	4.57	60.87	18.96	24.19	6.40	29.53	6.84
	HORVU1Hr1G094840			--	--	30.47	14.44	28.02	2.62	7.59	3.91	5.22	0.88
	HORVU3Hr1G067380			1.98	2.12	6.98	2.88	28.75	18.18	4.18	0.86	19.03	5.23
	HORVU7Hr1G029040			--	--	0.00	0.00	0.00	0.00	0.00	0.00	0.00	0.00
AT5G57050	refer AT4G26080	ABI2		--	--								

7 References

Aharoni, A., Dixit, S., Jetter, R., Thoenes, E., Arkel, G., & Pereira, A. (2004). The SHINE Clade of AP2 Domain Transcription Factors Activates Wax Biosynthesis, Alters Cuticle Properties, and Confers Drought Tolerance when Overexpressed in Arabidopsis. The Plant Cell 16, 2463–2480

Alexandersson, E., Fraysse, L., Sjövall-Larsen, S., Gustavsson, S., Fellert, M., Karlsson, M., Johanson, U., & Kjellbom, P. (2005). Whole gene family expression and drought stress regulation of aquaporins. Plant Molecular Biology 59, 469–484. https://doi.org/10.1007/s11103-005-0352-1

Almousa, M. (2017). Effect of high leaf temperature and nitrogen concentration on barley (*Hordeum vulgare L.*) photosynthesis and flowering. PhD Thesis, University of Glasgow.

Arentson, W. B., Sanyal, N., & Becker, F. D. (2013). Substrate channeling in proline metabolism. Frontiers in Bioscience 17, 375–388

Bargel, H., Koch, K., Cerman, Z., & Neinhuis, C. (2006). Structure-function relationships of the plant cuticle and cuticular waxes - A smart material? Functional Plant Biology 33, 893–910. https://doi.org/10.1071/FP06139

Basu, S., Ramegowda, V., Kumar, A., & Pereira, A. (2016). Plant adaptation to drought stress. F1000Research 5. https://doi.org/10.12688/F1000RESEARCH.7678.1

Basudeb, S. G., Vanaja, S. M., Lakshmi, J., & Maheswari, S. K. Y. M. (2019). Morpho-physiological and biochemical changes in black gram (Vigna mungo L . Hepper) genotypes under drought stress at flowering stage. Acta Physiologiae Plantarum 41, 1–14. https://doi.org/10.1007/s11738-019-2833-x

Bates, L. (1973). Rapid determination of free proline for water- stress studies. Plant and Soil 39, 205–207

Baxter, I., Hosmani, P. S., Rus, A., Lahner, B., Borevitz, J. O., Mickelbart, M. V, Schreiber, L., Franke, R. B., & Salt, D. E. (2009). Root Suberin Forms an Extracellular Barrier That Affects Water Relations and Mineral Nutrition in Arabidopsis. PLOS Genetics 5. https://doi.org/10.1371/journal.pgen.1000492

Bazihizina, N., Redwan, M., Taiti, C., Giordano, C., Monetti, E., Masi, E., Azzarello, E., & Mancuso, S. (2015). Root based responses account for Psidium guajava survival at high nickel concentration. Journal of Plant Physiology 174, 137–146. https://doi.org/10.1016/j.jplph.2014.10.011

Beisson, F., Li-beisson, Y., & Pollard, M. (2012). Solving the puzzles of cutin and suberin polymer biosynthesis. Current Opinion in Plant Biology 15, 329–337. https://doi.org/10.1016/j.pbi.2012.03.003

Bi, H., Kovalchuk, N., Langridge, P., Tricker, P. J., Lopato, S., & Borisjuk, N. (2017). The impact of drought on wheat leaf cuticle properties. BMC Plant Biology 17, 1–13. https://doi.org/10.1186/s12870-017-1033-3

Bi, H., Luang, S., Li, Y., Bazanova, N., Morran, S., Song, Z., Perera, M. A., Hrmova, M., Borisjuk, N., & Lopato, S. (2016). Identification and characterization of wheat drought-responsive MYB transcription factors involved in the regulation of cuticle biosynthesis. Journal of Experimental Botany 67, 5363–5380. https://doi.org/10.1093/jxb/erw298

Blee, E., & Schuber, F. (1993). Biosynthesis of cutin monomers: involvement of a lipoxygenase/peroxygenase pathway. The Plant Journalhe Plant Journal 4, 113–123.

Buschhaus, C., & Jetter, R. (2011). Composition differences between epicuticular and intracuticular wax substructures: How do plants seal their epidermal surfaces? Journal of Experimental Botany 62, 841–853. https://doi.org/10.1093/jxb/erq366

Campos, H., Cooper, M., Habben, J. E., Edmeades, G. O., & Schussler, J. R. (2004). Improving drought tolerance in maize: A view from industry. Field Crops Research 90, 19–34. https://doi.org/10.1016/j.fcr.2004.07.003

Century, K., Reuber, T. L., & Ratcliffe, O. J. (2008). Regulating the Regulators: The Future Prospects for Transcription-Factor-Based Agricultural Biotechnology Products. Plant Physiology 147, 20–29. https://doi.org/10.1104/pp.108.117887

Chaves, M. M., & Oliveira, M. M. (2004). Mechanisms underlying plant resilience to water deficits: Prospects for water-saving agriculture. Journal of Experimental Botany 55, 2365–2384. https://doi.org/10.1093/jxb/erh269

Chen, G., Komatsuda, T., Ma, J. F., et al. (2011). An ATP-binding cassette subfamily G full transporter is essential for the retention of leaf water in both wild barley and rice. Proceedings of the National Academy of Sciences 108, 12354–12359. https://doi.org/10.1073/pnas.1108444108

Chen, Guoxiong, Komatsuda, T., Ma, J. F., Li, C., Yamaji, N., & Nevo, E. (2011). A functional cutin matrix is required for plant protection against water loss. Plant Signaling and Behavior 6, 1297–1299. https://doi.org/10.4161/psb.6.9.17507

Daszkowska-Golec, A., & Szarejko, I. (2013). Open or Close the Gate – Stomata Action Under the Control of Phytohormones in Drought Stress Conditions. Frontiers in Plant Science 4, 1–16. https://doi.org/10.3389/fpls.2013.00138

Espelie, E. K., Bill, B., & Kolattukudy, P.(1979). Composition of Lipid-derived Polymers from Different Anatomical Regions of Several Plant Species. Plant Physiology 64, 1089–1093

Even, M., Sabo, M., Meng, D., Kreszies, T., Schreiber, L., & Fricke, W. (2018). Night-time transpiration in barley (Hordeum vulgare) facilitates respiratory carbon dioxide release and is regulated during salt stress. Annals of Botany 122, 569–582. https://doi.org/10.1093/aob/mcy084

Fich, E. A., Segerson, N. A., & Rose, J. K. C. (2016). The Plant Polyester Cutin: Biosynthesis, Structure, and Biological Roles. Annual Review of Plant Biology 67, 207–233. https://doi.org/10.1146/annurev-arplant-043015-111929

Franke, R., & Schreiber, L. (2007). Suberin - a biopolyester forming apoplastic plant interfaces. Current Opinion in Plant Biology 10, 252–259. https://doi.org/10.1016/j.pbi.2007.04.004

Giese, Bi. N. (1976). Roles of the cer-j and cer-p loci in determining the epicuticular wax composition on barley seedling leaves. Hereditas 82, 137–147. https://doi.org/10.1111/j.1601-5223.1976.tb01550.x

Gonzalez, A., & Ayerbe, L. (2010). Effect of terminal water stress on leaf epicuticular wax load , residual transpiration and grain yield in barley. Euphytica 172, 341–349. https://doi.org/10.1007/s10681-009-0027-0

Gunasekera, D., Santakumari, M., Glinka, Z., & Berkowitz, G. A. (1994). Wild and cultivated barley genotypes demonstrate varying ability to acclimate to plant water deficits. Plant Science 99, 125–134. https://doi.org/10.1016/0168-9452(94)90169-4

Heinen, R. B., & Ye, Q. (2009). Role of aquaporins in leaf physiology. Journal of Experimental Botany 60, 2971–2985. https://doi.org/10.1093/jxb/erp171

Hosy, E., Vavasseur, A., Mouline, K., Dreyer, I., Gaymard, F. de´ ric, Pore, F.,

Boucherez, J., Simonneau, T., Thibaud, J., Lebaudy, A., & Bouchez, D. (2003). The Arabidopsis outward K ⁺ channel GORK is involved in regulation of stomatal movements and plant transpiration. Proceedings of the National Academy of Sciences of the United States of America 100, 5549–5554

Islam, M. A., Du, H., Ning, J., Ye, H., & Xiong, L. (2009). Characterization of Glossy1-homologous genes in rice involved in leaf wax accumulation and drought resistance. Plant Molecular Biology 70, 443–456. https://doi.org/10.1007/s11103-009-9483-0

Jaleel, C. A., Manivannan, P., Wahid, A., Farooq, M., Al-Juburi, H. J., Somasundaram, R., & Pannerselvam, R. (2009). Drought Stress in Plants : A Review on Morphological Characteristics and Pigments Composition. International Journal of Agriculture and Biology 11, 100–105

Jang, J. Y., Kim, D. G., Kim, Y. O., Kim, J. S., & Kang, H. (2004). An expression analysis of a gene family encoding plasma membrane aquaporins in response to abiotic stresses in Arabidopsis thaliana. Plant Molecular Biology 54, 713–725. https://doi.org/10.1023/B:PLAN.0000040900.61345.a6

Jordan, W. R., Shouse, P. J., Blum, A., Miller, F. R., & Monk, R. L. (1984). Environmental Physiology of Sorghum. II. Epicuticular Wax Load and Cuticular Transpiration. Crop Science 24, 1168–1173

Kannangara, R., Branigan, C., Liu, Y., Penfield, T., Rao, V., Mouille, G., Höfte, H., Pauly, M., Riechmann, J. L., & Broun, P. (2007). The transcription factor WIN1/SHN1 regulates cutin biosynthesis in Arabidopsis thaliana. Plant Cell 19, 1278–1294. https://doi.org/10.1105/tpc.106.047076

Kapilan, R., Vaziri, M., & Zwiazek, J. J. (2018). Regulation of aquaporins in plants under stress. Biological Research 51, 1–11. https://doi.org/10.1186/s40659-018-0152-0

Kissinger, M., Tuvia-Alkalai, S., Shalom, Y., Fallik, E., Elkind, Y., Jenks, M. A., & Goodwin, M. S. (2005). Characterization of physiological and biochemical factors associated with postharvest water loss in ripe pepper fruit during storage. Journal of the American Society for Horticultural Science 130, 735–741. https://doi.org/10.21273/jashs.130.5.735

Kolattukudy, P. E. (1971). Enzymatic synthesis of fatty alcohols in Brassica oleracea. Archives of Biochemistry and Biophysics 142, 701–709. https://doi.org/10.1016/0003-9861(71)90536-4

Kosová, K., Vátámás, P., Urban, M. O., Kholová, J., & Prášil, I. T. (2014). Breeding for enhanced drought resistance in barley and wheat – drought-associated traits, genetic resources and their ptential uilization in beeding pogrammes. Czech Journal of Genetics and Plant Breeding 50, 247–261

Krauss, P., Markstädter, C., & Riederer, M. (1997). Attenuation of UV radiation by plant cuticles from woody species. Plant, Cell and Environment 20, 1079–1085. https://doi.org/10.1111/j.1365-3040.1997.tb00684.x

Kreszies, T., Eggels, S., Kreszies, V., Osthoff, A., Shellakkutti, N., Hochholdinger, F., Baldauf, J. A., Diehl, V. V. Z., Schreiber, L., & Ranathunge, K. (2020). Seminal roots of wild and cultivated barley differentially respond to osmotic stress in gene expression , suberization , and hydraulic conductivity. Plant Cell and Environment 43, 344–357. https://doi.org/10.1111/pce.13675

Kreszies, T., Shellakkutti, N., Osthoff, A., Yu, P., Baldauf, J. A., Zeisler-Diehl, V. V., Ranathunge, K., Hochholdinger, F., & Schreiber, L. (2019). Osmotic stress enhances suberization of apoplastic barriers in barley seminal roots: analysis of chemical, transcriptomic and physiological responses. New Phytologist. https://doi.org/10.1111/nph.15351

Kunst, L., & Samuels, A. L. (2003). Biosynthesis and secretion of plant cuticular wax. Progress in Lipid Research, 42(1), 51–80. https://doi.org/10.1002/ase.1798

Kusvuran, S. (2014). Effects of drought and salt stresses on growth , stomatal conductance , leaf water and osmotic potentials of melon genotypes (Cucumis melo L .). African Journal of Agricultural Research 7, 775/781. https://doi.org/10.5897/AJAR11.1783

Lakew, B., Eglinton, J., Henry, R. J., Baum, M., Grando, S., & Ceccarelli, S. (2011). The potential contribution of wild barley (Hordeum vulgare ssp. spontaneum) germplasm to drought tolerance of cultivated barley (H. vulgare ssp. vulgare). Field Crops Research 120, 161–168. https://doi.org/10.1016/j.fcr.2010.09.011

Larsson, S., & Svenningsson, M. (1986). Cuticular transpiration and epicuticular lipids of primary leaves of barley (Hordeum vulgare). Plant Physiology 68, 13–19

Law, C. W., Chen, Y., Shi, W., & Smyth, G. K. (2014). voom : precision weights unlock linear model analysis tools for RNA-seq read counts. Genome Biology 15, 1–17

Lee, S. B., & Suh, M. C. (2013). Recent advances in cuticular wax biosynthesis and its regulation in arabidopsis. Molecular Plant 6, 246–249. https://doi.org/10.1093/mp/sss159

Lian, H. L., Yu, X., Lane, D., Sun, W. N., Tang, Z. C., & Su, W. A. (2006). Upland rice and lowland rice exhibited different PIP expression under water deficit and ABA treatment. Cell Research 16, 651–660. https://doi.org/10.1038/sj.cr.7310068

Liu, N., Chen, J., Wang, T., Li, Q., Cui, P., Jia, C., & Hong, Y. (2019). Overexpression of WAX INDUCER1/SHINE1 gene enhances wax accumulation under osmotic stress and oil synthesis in Brassica napus. International Journal of Molecular Sciences 20, 1–16. https://doi.org/10.3390/ijms20184435

Lockhart, J. A. (1965). An Analysis of Irreversible Plant Cell Elongation. Jounal of Theoretical Biology 8, 264–275

Long, S. P., & Ort, D. R. (2010). More than taking the heat: Crops and global change. Current Opinion in Plant Biology 13, 241–248. https://doi.org/10.1016/j.pbi.2010.04.008

Lu, S., Song, T., Kosma, D. K., Parsons, E. P., Rowland, O., & Jenks, M. A. (2009). Arabidopsis CER8 encodes LONG-CHAIN ACYL-COA SYNTHETASE 1 (LACS1) that has overlapping functions with LACS2 in plant wax and cutin synthesis. The Plant Journale Plant Journal 59, 553–564. https://doi.org/10.1111/j.1365-313X.2009.03892.x

Lulai, E., Corsini, D., & Crop, N. (1998). Differential deposition of suberin phenolic and aliphatic domains and their roles in resistance to infection during potato tuber (*Solanum tuberosum L* .) wound-healing. Physiological and Molecular Plant Pathology 53, 209–222. https://doi.org/10.1006/pmpp.1998.0179

Mascher, M., Gundlach, H., Himmelbach, A., et al. (2017). A chromosome conformation capture ordered sequence of the barley genome. Nature 544, 427–433.https://doi.org/10.1038/nature22043

Michel, B. E. (1983). Evaluation of the Water Potentials of Solutions of Polyethylene Glycol 8000 Both in the Absence and Presence of Other Solutes. Plant Physiology 72, 66–70. https://doi.org/0032-0889/83/72/0066/05/$00.50/0

Miyashita, K., Tanakamaru, S., Maitani, T., & Kimura, K. (2005). Recovery responses of photosynthesis , transpiration , and stomatal conductance in kidney bean following drought stress. Environmental and Experimental Botany 53, 205–214. https://doi.org/10.1016/j.envexpbot.2004.03.015

Moshelion, M., Halperin, O., Wallach, R., Oren, R., & Way, D. A. (2015). Role of aquaporins in determining transpiration and photosynthesis in water-stressed plants: Crop water-use efficiency, growth and yield. Plant, Cell and Environment 38, 1785–1793.

https://doi.org/10.1111/pce.12410

Müller, C., & Riederer, M. (2005). Plant surface properties in chemical ecology. Journal of Chemical Ecology 31, 2621–2651. https://doi.org/10.1007/s10886-005-7617-7

Murata, N., Allakhverdiev, S. I., & Nishiyama, Y. (2012). The mechanism of photoinhibition in vivo: Re-evaluation of the roles of catalase, α-tocopherol, non-photochemical quenching, and electron transport. Biochimica et Biophysica Acta - Bioenergetics 1817, 1127–1133. https://doi.org/10.1016/j.bbabio.2012.02.020

Muzammil, S., Shrestha, A., Dadshani, S., Pillen, K., Siddique, S., & Léon, J. (2018). An Ancestral Allele of Pyrroline-5-carboxylate synthase1 Promotes Proline Accumulation and Drought Adaptation in. Plant Physiology 178, 771–782. https://doi.org/10.1104/pp.18.00169

Nazarli, H., & Faraji, F. (2011). Response of proline , soluble sugars and antioxidant enzymes in wheat (*Triticum aestivum l* .) to different irrigation regimes in greenhouse condition. Cercetări Agronomice În Moldova 44

Neumann, M., Azaizeh, H., & Leon, D. (1994). Hardening of root cell walls : a growth inhibitory response to salinity stress. Plant, Cell and Environment 17, 303–309.

Niederl, S., Kirsch, T., Riederer, M., & Schreiber, L. (1998). Co-Permeability of 3 H-Labeled Water and 14 C-Labeled Organic Acids across Isolated Plant Cuticles . Plant Physiology 116, 117–123. https://doi.org/10.1104/pp.116.1.117

Nonami, H., & Boyer, J. S. (1990). Wall Extensibility and Cell Hydraulic Conductivity Decrease in Enlarging Stem Tissues at Low Water Potentials. Plant Physiology, 93, 1610–1619

Oliverira, A. B., Alencer, M., & Gomes-Filho. (2013). Comparison Between the Water and Salt Stress Effects on Plant Growth and Development Alexandre. Intechopen, 67–94. https://doi.org/http://dx.doi.org/10.5772/54223

Ooi, A., Lemtiri-Chlieh, F., Wong, A., & Gehring, C. (2017). Direct Modulation of the Guard Cell Outward-Rectifying Potassium Channel (GORK) by Abscisic Acid. Molecular Plant 10, 1469–1472. https://doi.org/10.1016/j.molp.2017.08.010

Orata, F. (2012). Derivatization Reactions and Reagents for Gas Chromatography Analysis. Advanced Gas Chromatography - Progress in Agricultural, Biomedical and Industrial Applications, 83–156. https://doi.org/10.5772/33098

Osthoff, A., Donà Dalle Rose, P., Baldauf, J. A., Piepho, H. P., & Hochholdinger, F. (2019). Transcriptomic reprogramming of barley seminal roots by combined water deficit and salt stress. BMC Genomics 20, 1–14. https://doi.org/10.1186/s12864-019-5634-0

Panikashvili, D., Shi, J. X., Schreiber, L., & Aharoni, A. (2009). The arabidopsis DCR encoding a soluble BAHD acyltransferase is required for cutin polyester formation and seed hydration properties. Plant Physiology 151, 1773–1789. https://doi.org/10.1104/pp.109.143388

Perrone, I., Gambino, G., Chitarra, W., Vitali, M., Pagliarani, C., Riccomagno, N., Balestrini, R., Kaldenhoff, R., Uehlein, N., Gribaudo, I., Schubert, A., & Lovisolo, C. (2012). The grapevine root-specific aquaporin VvPIP2;4N controls root hydraulic conductance and leaf gas exchange under well-watered conditions but not under water stress. Plant Physiology 160, 965–977. https://doi.org/10.1104/pp.112.203455

Raison, K. J. (1980). Membrane Lipids: Structure and Function. In P.Stumpf eds, Lipids: Structure and Function. Academic Press

Ranathunge, K., Schreiber, L., & Franke, R. (2011). Suberin research in the genomics era-New interest for an old polymer. Plant Science, 180(3), 339–413. https://doi.org/10.1016/j.plantsci.2010.11.003

Richardson, A., Franke, R., Kerstiens, G., Jarvis, M., Schreiber, L., & Fricke, W. (2005). Cuticular wax deposition in growing barley (Hordeum vulgare) leaves commences in relation to the point of emergence of epidermal cells from the sheaths of older leaves. Planta 222, 472–483. https://doi.org/10.1007/s00425-005-1552-2

Richardson, A., Wojciechowski, T., Franke, R., Schreiber, L., Kerstiens, G., Jarvis, M., & Fricke, W. (2007). Cuticular permeance in relation to wax and cutin development along the growing barley (Hordeum vulgare) leaf. Planta 225, 1471–1481. https://doi.org/10.1007/s00425-006-0456-0

Ritchie, M. E., Phipson, B., Wu, D., Hu, Y., Law, C. W., Shi, W., & Smyth, G. K. (2015). limma powers differential expression analyses for RNA-sequencing and microarray studies. Nucleic Acids Research 43, 1–13. https://doi.org/10.1093/nar/gkv007

Rowland, O., Zheng, H., Hepworth, S. R., Lam, P., Jetter, R., & Kunst, L. (2006). CER4 encodes an alcohol-forming fatty acyl-coenzyme A reductase involved in cuticular wax production in Arabidopsis. Plant Physiology 142, 866–877 https://doi.org/10.1104/pp.106.086785

Sallam, A., Alqudah, A. M., Dawood, M. F. A., Baenziger, P. S., & Börner, A. (2019). Drought Stress Tolerance in Wheat and Barley : Advances in Physiology , Breeding and Genetics Research. International Journal of Molecular Sciences 20, 1–36.

Sanchez, F., Manzanares, M., Andres, E., Tenorio, L., & Ayerbe, L. (2001). Residual transpiration rate , epicuticular wax load and leaf colour of pea plants in drought conditions . Influence on harvest index and canopy temperature. European Journal of Agronomy 15, 57–70

Schönherr, J. (2006). Characterization of aqueous pores in plant cuticles and permeation of ionic solutes. Journal of Experimental Botany 57, 2471–2491. https://doi.org/10.1093/jxb/erj217

Schreiber, L. (2010). Transport barriers made of cutin, suberin and associated waxes. Trends in Plant Science 15, 546–553. https://doi.org/10.1016/j.tplants.2010.06.004

Schreiber, L., & Riederer, M. (1996). Ecophysiology of cuticular transpiration : comparative investigation of cuticular water permeability of plant species from different habitats. Oecologia 107, 426–432

Selvakumar, G., Panneerselvam, P., & Ganeshamurthy, N. A. (2012). Bacterial Mediated Alleviation of Abiotic Stress in Crops. In D. Maheshwari eds, Bacteria in Agrobiology: Stress Management. https://doi.org/https://doi.org/10.1007/978-3-642-23465-1_10

Smyth, G. K. (2004). Linear Models and Empirical Bayes Methods for Assessing Differential Expression in Microarray Experiments Linear Models and Empirical Bayes Methods for Assessing Differential Expression in Microarray Experiments. Statistical Applications in Genetics and Molecular Biology 3. https://doi.org/10.2202/1544-6115.1027

Solovchenko, A., & Merzlyak, M. (2003). Optical properties and contribution of cuticle to UV protection in plants: Experiments with apple fruit. Photochemical and Photobiological Sciences 2, 861–866. https://doi.org/10.1039/b302478d

Steudle, E. (2000). Water uptake by roots: an integration of views. Plant Soil 226, 45–56

Svenningsson, M. (1988). Epi- and intracuticular lipids and cuticular transpiration rates of

primary leaves of eight barley (*Hordeum vulgare*) cultivars. Physiologia Plantarum 73, 512–517

Tanaka, T., Tanaka, H., Machida, C., Watanabe, M., & Machida, Y. (2004). A new method for rapid visualization of defects in leaf cuticle reveals five intrinsic patterns of surface defects in Arabidopsis. Plant Journal 37, 139–146. https://doi.org/10.1046/j.1365-313X.2003.01946.x

Turan, M. A., Hassan, A., Elkarim, A., Taban, N., & Taban, S. (2009). Effect of salt stress on growth , stomatal resistance , proline and chlorophyll concentrations on maize plant. African Journal of Agricultural Research 49, 893–897

Turner, N. C., Begg, J. E., & Tonnet, M. L. (1978). Osmotic Adjustment of Sorghum and Sunflower Crops in Response to Water Deficits and Its Influence on the Water Potential at Which Stomata Close. Australian Journal of Plant Physiology 5, 597–608. https://doi.org/10.1071/PP9780597

Turner, & Singh, D. (1984). Responses of Adaxial and Abaxial Stomata to Light and Water Deficits in Sunflower and Sorghum. New Phytologist 96, 187–195

Vogg, G., Fischer, S., Leide, J., Emmanuel, E., Jetter, R., Levy, A. A., & Riederer, M. (2004). Tomato fruit cuticular waxes and their effects on transpiration barrier properties : functional characterization of a mutant deficient in a very-long-chain fatty acid b -ketoacyl-CoA synthase. Journal of Experimental Botany 55, 1401–1410. https://doi.org/10.1093/jxb/erh149

Wang, M., Wang, Y., Wu, H., Xu, J., Li, T., Hegebarth, D., Jetter, R., Chen, L., & Wang, Z. (2016). Three TaFAR genes function in the biosynthesis of primary alcohols and the response to abiotic stresses in Triticum aestivum. Scientific Reports 6, 1–14. https://doi.org/10.1038/srep25008

Wang, X., Wu, W., & Assmann, S. M. (1998). Differential Responses of Abaxial and Adaxial Guard Cells of Broad Bean to Abscisic Acid and Calcium. Plant Physiology 118, 1421–1429

Wang, Y., Jin, S., Xu, Y., Li, S., Zhang, S., Yuan, Z., Li, J., & Ni, Y. (2020). Overexpression of BnKCS1-1, BnKCS1-2, and BnCER1-2 promotes cuticular wax production and increases drought tolerance in Brassica napus. Crop Journal 8, 26–37. https://doi.org/10.1016/j.cj.2019.04.006

Wettstein-Knowels, P.(1993). Waxes, cutin, and suberin. In: J. Moore, S.Thomas eds, Lipid Metabolism in Plants. CRC revivals. https://doi.org/10.1201/9781351074070

Xue, D., Zhang, X., Lu, X., Chen, G., Chen, Z., & Chen, Z. (2017). Molecular and Evolutionary Mechanisms of Cuticular Wax for Plant Drought Tolerance. Frontiers in Plant Scienc, 8, 1–12. https://doi.org/10.3389/fpls.2017.00621

Yang, W., Simpson, J. P., Li-Beisson, Y., Beisson, F., Pollard, M., & Ohlrogge, J. B. (2012). A land-plant-specific glycerol-3-phosphate acyltransferase family in arabidopsis: Substrate specificity, sn-2 preference, and evolution. Plant Physiology 160, 638–652. https://doi.org/10.1104/pp.112.201996

Yeats, T. H., & Rose, J. K. C. (2013). The formation and function of plant cuticles. Plant Physiology 163, 5–20. https://doi.org/10.1104/pp.113.222737

Yeo, A. R., Caporn, S. J. M., & Flowers, T. J. (1985). The Effect of Salinity upon Photosynthesis in Rice (*Oryza sativa L* .): Gas Exchange by Individual Leaves in relation to their Salt Content. Journal of Developmental Biology 36, 1240–1248.

Zabka, V. (2007). The Plasticity of Barley (Hordeum vulgare) Leaf Wax Characteristics and their Effects on Early Events in the Powdery Mildew Fungus (*Blumeria graminis f* . sp . hordei): Interactive Adaptations at the Physiological and the Molecular Level. PhD thesis, Julius-Maximilians-Universität Würzburg

Zeier Jurgen, & Schreiber, L. (1997). Chemical Composition of Hypodermal and Endodermal Cell Walls and Xylem Vessels Isolated from Clivia miniata. Plant Physiology 113, 1223–1231

Zeisler, V., Migdal, B., & Schreiber, L. (2017). Quantitative characterization of cuticular barrier properties: methods, requirements, and problems. Journal of Experimental Botany 68, 5281–5291. https://doi.org/10.1093/jxb/erx282

Zeisler, V., Müller, Y., & Schreiber, L. (2018). Epicuticular wax on leaf cuticles does not establish the transpiration barrier, which is essentially formed by intracuticular wax. Journal of Plant Physiology 227, 66–74. https://doi.org/10.1016/j.jplph.2018.03.018

Zeisler, V., & Schreiber, L. (2016). Epicuticular wax on cherry laurel (*Prunus laurocerasus*) leaves does not constitute the cuticular transpiration barrier. Planta 243, 65–81. https://doi.org/10.1007/s00425-015-2397-y

Zhang, J. Y., Broeckling, C. D., Blancaflor, E. B., Sledge, M. K., Sumner, L. W., & Wang, Z. Y. (2005). Overexpression of WXP1, a putative Medicago truncatula AP2 domain-containing transcription factor gene, increases cuticular wax accumulation and enhances drought tolerance in transgenic alfalfa (*Medicago sativa*). Plant Journal 42, 689–707

https://doi.org/10.1111/j.1365-313X.2005.02405.x

Ziv, C., Zhao, Z., Gao, Y. G., & Xia, Y. (2018). Multifunctional roles of plant cuticle during plant-pathogen interactions. Frontiers in Plant Science 9, 1–8. https://doi.org/10.3389/fpls.2018.01088

8 Acknowledgement

I would like to express my special gratitude and greatfullness to Prof. Dr Lukas Schreiber for encouraging me to continue in his research group for my doctorate studies. His doors were always open for discussions and clarifying doubts. His immense support during the work on this thesis was very helpful for the completion of my doctorate.

My heartfelt and special thank you goes to Dr. Tino Kreszies for guiding and teaching me all the techniques involved in the thesis.

I thank Prof. Dr. Frank Hochholdinger and his colleague Anika for supporting transcriptomics data and Prof. Dr. Jens Leon, PD Dr. Ali Naz and Mrs. Karola Müller for providing the barley seeds.

Special thanks to all my colleagues for giving me a pleasant atmosphere in the research group and for fun gatherings.

Thanks to my friend and colleague Priya for all the time we spent together in lab and fun time searching for a nice ice coffee.

Last but not the least, my thankfulness and appreciation goes to my family for the constant support they gave me throughout my work.